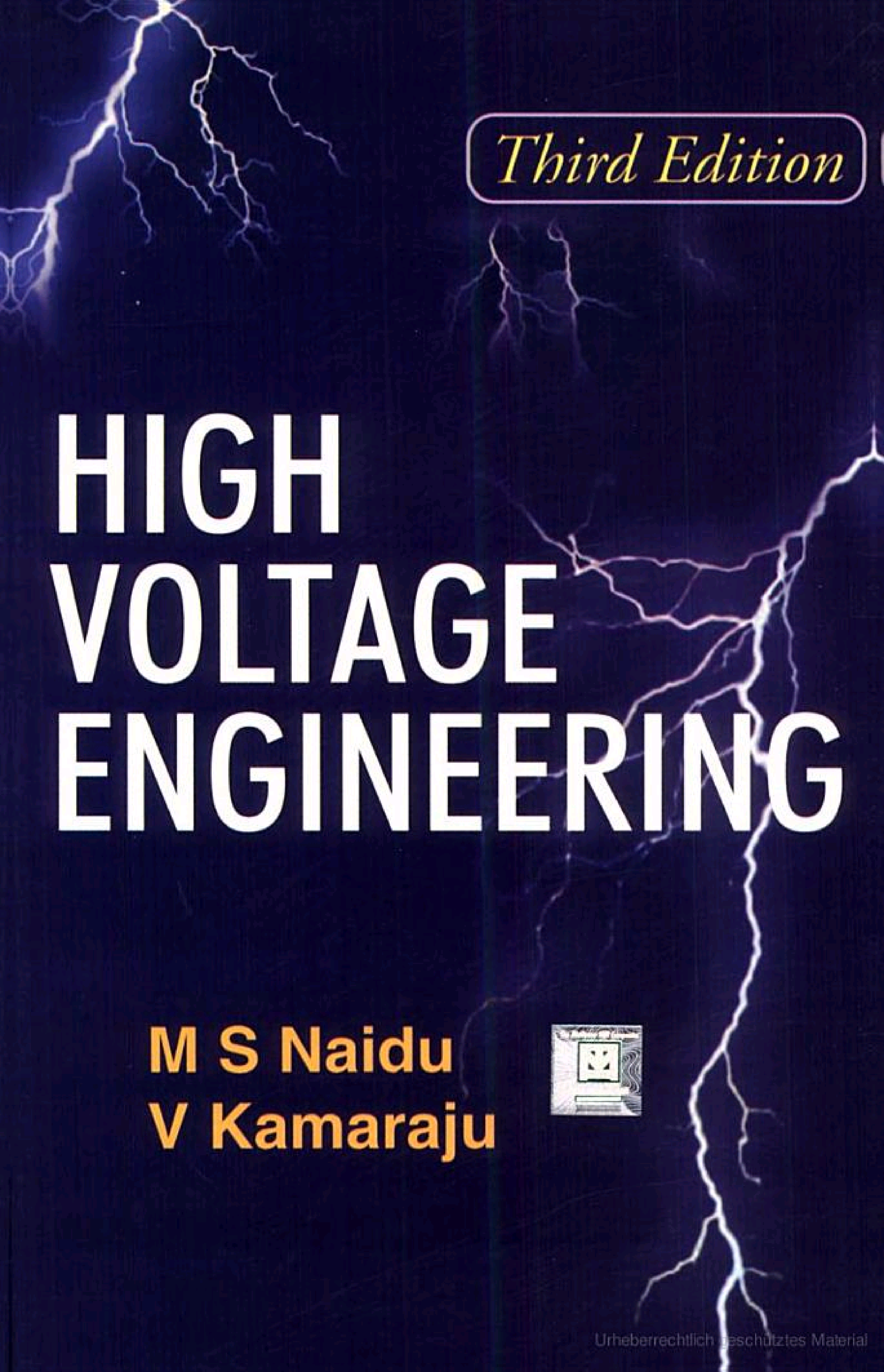

Third Edition

HIGH VOLTAGE ENGINEERING

M S Naidu
V Kamaraju

Information contained in this work has been obtained by Tata McGraw-Hill, from sources believed to be reliable. However, neither Tata McGraw-Hill nor its authors guarantee the accuracy or completeness of any information published herein, and neither Tata McGraw-Hill nor its authors shall be responsible for any errors, omissions, or damages arising out of use of this information. This work is published with the understanding that Tata McGraw-Hill and its authors are supplying information but are not attempting to render engineering or other professional services. If such services are required, the assistance of an appropriate professional should be sought.

Tata McGraw-Hill

Copyright © 2004, 1995, by Tata McGraw-Hill Publishing Company Limited.

Tenth reprint 2006
RQLDRRBKRZRAR

No part of this publication may be reproduced or distributed in any form or by any means, electronic, mechanical, photocopying, recording, or otherwise or stored in a database or retrieval system without the prior written permission of the publishers. The program listings (if any) may be entered, stored and executed in a computer system, but they may not be reproduced for publication.

This edition can be exported from India only by the publishers,
Tata McGraw-Hill Publishing Company Limited.

ISBN 0-07-049464-9

Published by the Tata McGraw-Hill Publishing Company Limited,
7 West Patel Nagar, New Delhi 110 008, Typeset at Script Makers,
19, A1-B, DDA Market, Paschim Vihar, New Delhi 110 063 and printed at
Adarsh Printers, Naveen Shahdara, Delhi 110 032.

Cover: Pushp Print Services

The McGraw·Hill Companies

Urheberrechtlich geschütztes Material

Contents

1

Introduction

In modern times, high voltages are used for a wide variety of applications covering the power systems, industry, and research laboratories. Such applications have become essential to sustain modern civilization. High voltages are applied in laboratories in nuclear research, in particle accelerators, and Van de Graaff generators. For transmission of large bulks of power over long distances, high voltages are indispensable. Also, voltages up to 100 kV are used in electrostatic precipitators, in automobile ignition coils, etc. X-ray equipment for medical and industrial applications also uses high voltages. Modern high voltage test laboratories employ voltages up to 6 MV or more. The diverse conditions under which a high voltage apparatus is used necessitate careful design of its insulation and the electrostatic field profiles. The principal media of insulation used are gases, vacuum, solid, and liquid, or a combination of these. For achieving reliability and economy, a knowledge of the causes of deterioration is essential, and the tendency to increase the voltage stress for optimum design calls for judicious selection of insulation in relation to the dielectric strength, corona discharges, and other relevant factors. In this chapter some of the general principles used in high voltage technology are discussed.

1.1 | ELECTRIC FIELD STRESSES

Like in mechanical designs where the criterion for design depends on the mechanical strength of the materials and the stresses that are generated during their operation, in high voltage applications, the dielectric strength of insulating materials and the electric field stresses developed in them when subjected to high voltages are the important factors in high voltage systems. In a high voltage apparatus the important materials used are conductors and insulators. While the conductors carry the current, the insulators prevent the flow of currents in undesired paths. The electric stress to which an insulating material is subjected to is numerically equal to the voltage gradient, and is equal to the electric field intensity,

$$\mathbf{E} = -\nabla\varphi \tag{1.1}$$

where **E** is the electric field intensity, φ is the applied voltage, and ∇ (read del) operator is defined as

$$\nabla = a_x \frac{\partial}{\partial x} + a_y \frac{\partial}{\partial y} + a_z \frac{\partial}{\partial z}$$

where a_x, a_y, and a_z are components of position vector $\mathbf{r} = a_x\,\mathbf{x} + a_y\,\mathbf{y} + a_z\mathbf{z}$.

As already mentioned, the most important material used in a high voltage apparatus is the insulation. The dielectric strength of an insulating material can be defined as the maximum dielectric stress which the material can withstand. It can also be defined as the voltage at which the current starts increasing to very high values unless controlled by the external impedance of the circuit. The electric breakdown strength of insulating materials depends on a variety of parameters, such as pressure, temperature, humidity, field configurations, nature of applied voltage, imperfections in dielectric materials, material of electrodes, and surface conditions of electrodes, etc. An understanding of the failure of the insulation will be possible by the study of the possible mechanisms by which the failure can occur.

The most common cause of insulation failure is the presence of discharges either within the voids in the insulation or over the surface of the insulation. The probability of failure will be greatly reduced if such discharges could be eliminated at the normal working voltage. Then, failure can occur as a result of thermal or electrochemical deterioration of the insulation.

1.2 | GAS/VACUUM AS INSULATOR

Air at atmospheric pressure is the most common gaseous insulation. The breakdown of air is of considerable practical importance to the design engineers of power transmission lines and power apparatus. Breakdown occurs in gases due to the process of collisional ionization. Electrons get multiplied in an exponential manner, and if the applied voltage is sufficiently large, breakdown occurs. In some gases, free electrons are removed by attachment to neutral gas molecules; the breakdown strength of such gases is substantially large. An example of such a gas, with larger dielectric strength, is sulphur hexafluoride (SF_6).

High pressure gas provides a flexible and reliable medium for high voltage insulation. Using gases at high pressures, field gradients up to 25 MV/m have been realized. Nitrogen (N_2) was the gas first used at high pressures because of its inertness and chemical stability, but its dielectric strength is the same as that of air. Other important practical insulating gases are carbon dioxide (CO_2), dichlorodifluoromethane (CCl_2F_2) (popularly known as freon), and sulphur hexafluoride (SF_6). The breakdown voltage at higher pressures in gases shows an increasing dependence on the nature and smoothness of the electrode material. It is relevant to point out that, of the gases examined to-date, SF_6 has probably the most attractive overall dielectric and arc quenching properties for gas insulated high voltage systems.

However, in recent years pure SF_6 gas has been found to be a green house gas causing environmental hazards and therefore research efforts are presently focussed on finding a replacement gas or gas mixture which is environmentally friendly. Pure nitrogen, air and SF_6/N_2 mixtures show good potential to replace SF_6 gas in high voltage apparatus. In the next few years, SF_6/N_2, SF_6 gas has to be replaced by a new gas and lot of research is being done to find such a gas.

Ideally, vacuum is the best insulator with field strengths up to 10^7 V/cm, limited only by emissions from the electrode surfaces. This decreases to less than 10^5 V/cm for gaps of several centimetres. Under high vacuum conditions, where the pressures are below 10^{-4} torr*, the breakdown cannot occur due to collisional processes like in gases, and hence the breakdown strength is quite high. Vacuum insulation is used in particle accelerators, x-ray and field emission tubes, electron microscopes, capacitors, and circuit breakers.

1.3 | LIQUID DIELECTRICS

Liquids are used in high voltage equipment to serve the dual purpose of insulation and heat condition. They have the advantage that a puncture path is self-healing. Temporary failures due to overvoltage are reinsulated quickly by liquid flow to the attacked area. However, the products of the discharges may deposit on solid insulation supports and may lead to surface breakdown over these solid supports.

Highly purified liquids have dielectric strengths as high as 1 MV/cm. Under actual service conditions, the breakdown strength reduces considerably due to the presence of impurities. The breakdown mechanism in the case of very pure liquids is the same as the gas breakdown, but in commercial liquids, the breakdown mechanisms are significantly altered by the presence of the solid impurities and dissolved gases.

Petroleum oils are the commonest insulating liquids. However, fluorocarbons, silicones, and organic esters including castor oil are used in significant quantities. A number of considerations enter into the selection of any dielectric liquid. The important electrical properties of the liquid include the dielectric strength, conductivity, flash point, gas content, viscosity, dielectric constant, dissipation factor, stability, etc. Because of their low dissipation factor and other excellent characteristics, polybutanes are being increasingly used in the electrical industry. However, in 1970s it was found that Askarels which more extensively used, exhibit health hazards and therefore most countries have legally banned their production and use. Many new liquids have since been developed which have no adverse environmental hazards. These include silicone oils, synthetic and fluorinated hydrocarbons.

In practical applications liquids are normally used at voltage stresses of about 50–60 kV/cm when the equipment is continuously operated. On the other hand, in applications like high voltage bushings, where the liquid only fills up the voids in the solid dielectric, it can be used at stresses as high as 100–200 kV/cm.

---

* 1 torr = 1 mm of Hg.

1.4 | SOLIDS AND COMPOSITES

1.4.1 Solid Dielectrics

A good solid dielectric should have some of the properties mentioned earlier for gases and liquids and it should also possess good mechanical and bonding strengths. Many organic and inorganic materials are used for high voltage insulation purposes. Widely used inorganic materials are ceramics and glass. The most widely used organic materials are thermosetting epoxy resins such as polyvinyl chloride (PVC), polyethylene (PE) or cross linked polyethylene (XLPE). Kraft paper, natural rubber, silicon rubber and polypropylene rubber are some of the other materials widely used as insulants in electrical equipment.

If the solid insulating material is truly homogeneous and is free from imperfections, its breakdown stress will be as high as 10 MV/cm. This is the 'intrinsic breakdown strength', and can be obtained only under carefully controlled laboratory conditions. However, in practice, the breakdown fields obtained are very much lower than this value. The breakdown occurs due to many mechanisms. In general, the breakdown occurs over the surface than in the solid itself, and the surface insulation failure is the most frequent cause of trouble in practice.

1.4.2 Composites

In many engineering applications, more than one types of insulation are used together, mainly in parallel, giving rise to composite insulation systems. Examples of such systems are solid/gas insulation (transmission line insulators), solid/vacuum insulation and solid/liquid composite insulation systems (transformer winding insulation, oil impregnated paper and oil impregnated metallised plastic film etc).

In the application of composites, it is important to make sure that both the components of the composite should be chemically stable and will not react with each other under the application of combined thermal, mechanical and electrical stresses over the expected life of the equipment. They should also have nearly equal dielectric constants. Further, the liquid insulant should not absorb any impurities from the solid, which may adversely affect its resistivity, dielectric strength, loss factor and other properties of the liquid dielectric.

It is the intensity of the electric field that determines the onset of breakdown and the rate of increase of current before breakdown. Therefore, it is very essential that the electric stress should be properly estimated and its distribution known in a high voltage apparatus. Special care should be exercised in eliminating the stress in the regions where it is expected to be maximum, such as in the presence of sharp points.

1.5 | ESTIMATION AND CONTROL OF ELECTRIC STRESS

The electric field distribution is usually governed by the Poisson's equation:

$$\nabla^2 \varphi = -\frac{\rho}{\varepsilon_0} \tag{1.2}$$

where φ is the potential at a given point, ρ is the space charge density in the region, and ε_0 is the electric permittivity of free space (vacuum). However, in most of the high voltage apparatus, space charges are not normally present, and hence the potential distribution is governed by the Laplace's equation:

$$\nabla^2 \varphi = 0 \tag{1.3}$$

In Eqs (1.2) and (1.3) the operator ∇^2 is called the Laplacian and is a vector with properties

$$\nabla \cdot \nabla = \nabla^2 = \frac{\partial^2}{\partial x^2} + \frac{\partial^2}{\partial y^2} + \frac{\partial^2}{\partial z^2}$$

There are many methods available for determining the potential distribution. The most commonly used methods are

(i) the electrolytic tank method, and
(ii) the numerical methods

The potential distribution can also be calculated directly. However, this is very difficult except for simple geometries. In many practical cases, a good understanding of the problem is possible by using some simple rules to plot the field lines and equipotentials. The important rules are

(i) the equipotentials cut the field lines at right angles,
(ii) when the equipotentials and field lines are drawn to form curvilinear squares; the density of the field lines is an indication of the electric stress in a given region, and
(iii) in any region, the maximum electric field is given by *dv*/*dx*, where *dv* is the voltage difference between two successive equipotentials, *dx* apart.

Considerable amount of labour and time can be saved by properly choosing the planes of symmetry and shaping the electrodes accordingly. Once the voltage distribution of a given geometry is established, it is easy to refashion or redesign the electrodes to minimize the stresses so that the onset of corona is prevented. This is a case normally encountered in high voltage electrodes of the bushings, standard capacitors, etc. When two dielectrics of widely different permittivities are in series, the electric stress is very much higher in the medium of lower permittivity. Considering a solid insulation in a gas medium, the stress in the gas becomes ε_r times that in the solid dielectric, where ε_r is the relative permittivity of the solid dielectric. This enhanced stress occurs at the electrode edges and one method of overcoming this is to increase the electrode diameter. Other methods of stress control are shown in Fig. 1.1.

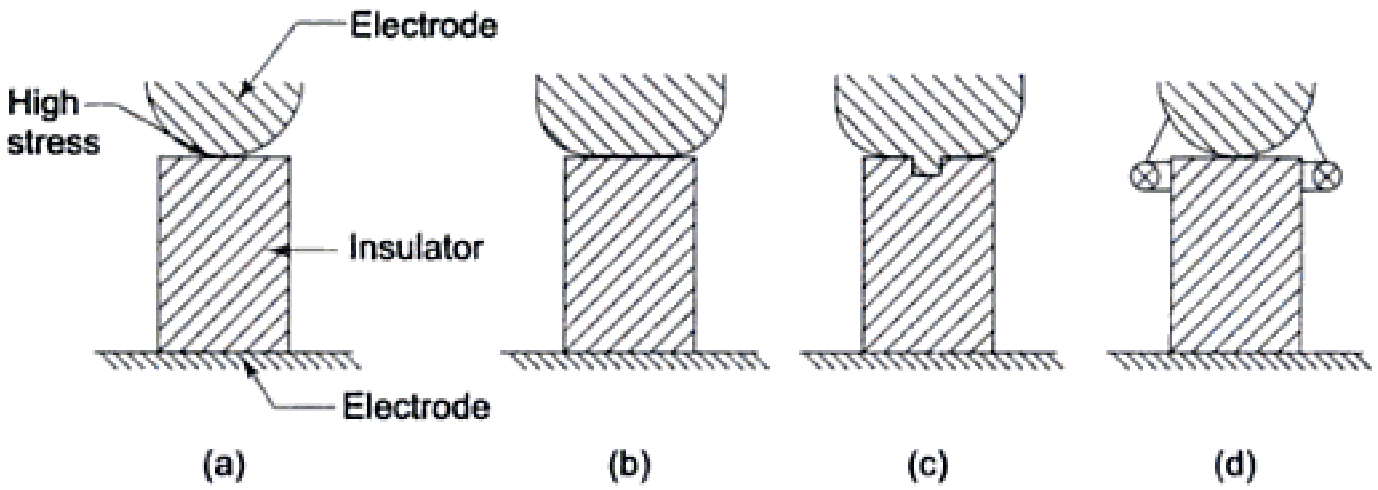

Fig. 1.1 *Control of stress at an electrode edge*

In the design of high voltage apparatus, the electric field intensities have to be controlled, otherwise higher stresses will trigger or accelerate the aging of the insulation leading to its failure. Over the years, many methods for controlling and optimizing electric fields to get the most economical designs have been developed. Electric field control methods form an important component of the overall design of equipment.

1.5.1 Electric Field

A brief review of the concepts of electric fields is presented, as it is essential for high voltage engineers to have a knowledge of the field intensities in various media under electric stresses. It also helps in choosing proper electrode configurations and economical dimensioning of the insulation, such that highly stressed regions are not formed and reliable operation of the equipment results in its anticipated life.

The field intensity **E** at any location in an electrostatic field is the ratio of the force on an infinitely small charge at that location to the charge itself as the charge decreases to zero. The force **F** on any charge q at that point in the field is given by

$$\mathbf{F} = q\,\mathbf{E} \tag{1.4}$$

The electric flux density **D** associated with the field intensity **E** is

$$\mathbf{D} = \varepsilon\,\mathbf{E} \tag{1.5}$$

where ε is the permittivity of the medium in which the electric field exists. The work done on a charge when moved in an electric field is defined as the potential. The potential φ is equal to

$$\varphi = -\int_{l} \mathbf{E}\cdot d\mathbf{l} \tag{1.6}$$

where l is the path through which the charge is moved.

Several relationships between the various quantities in the electric field can be summarized as follows:

$$\mathrm{D} = \varepsilon\,\mathbf{E} \tag{1.5}$$

$$\varphi = -\int_l \mathbf{E}\cdot d\mathbf{l} \,(\text{or } \mathbf{E} = -\nabla\varphi) \tag{1.6}$$

$$\mathbf{E} = \frac{\mathbf{F}}{q} \tag{1.7}$$

$$\iint_S \mathbf{E}\cdot d\mathbf{S} = \frac{q}{\varepsilon_0} \text{ (Gauss theorem)} \tag{1.8}$$

$$\nabla \cdot \mathbf{D} = \rho \text{ (Charge density)} \tag{1.9}$$

$$\nabla^2 \varphi = -\frac{\rho}{\varepsilon_0} \text{ (Poisson's equation)} \tag{1.10}$$

$$\nabla^2 \varphi = 0 \text{ (Laplace's equation)} \tag{1.11}$$

where **F** is the force exerted on a charge q in the electric field **E**, and **S** is the closed surface containing charge q.

1.5.2 Uniform and Non-Uniform Electric Fields

In general, the electric fields between any two electrodes can be either uniform and non-uniform. In a uniform field gap, the average field **E** is the same throughout the field rigion, whereas in a non-uniform field gap, **E** is different at different points of the field region.

Uniform or approximately uniform field distributions exist between two infinite parallel plates or two spheres of equal diameters when the gap distance is less than diameter of the sphere. Spherical electrodes are frequently used for high voltage measurements and for triggering in impulse voltage generation circuits. Sometimes, parallel plates of finite size are used to simulate uniform electric fields, when gap separation is much smaller than plate size.

In the absence of space charges, the average field **E** in a non-uniform field gap is maximum at the surface of the conductor which has the smallest radius of curvature. It has the minimum field **E** at the conductor having the large radius of curvature. In this case, the field is not only non-uniform but also asymmetrical. Most of the practical high voltage components used in electric power systems normally have non-uniform and asymmetrical field distribution.

1.5.3 Estimation of Electric Field in Some Geometric Boundaries

It has been shown that the maximum electric field E_m in a given electric field configuration is of importance. The mean electric field over a distance d between two conductors with a potential difference of V_{12} is

$$E_{av} = \frac{V_{12}}{d} \tag{1.12}$$

In field configurations of non-uniform fields, the maximum electric field E_m is always higher than the average value. For some common field configurations, the maximum value of E_m and the field enhancement factor f given by E_m/E_{av} are presented in Table 1.1.

Table 1.1 *Some Geometrical Configurations and the Field Factors*

Geometrical configuration	*Maximum electric field* E_m	*Field enhancement factor* $f = E_m/E_{av}$
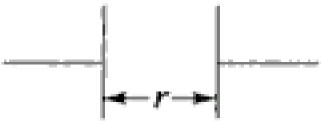 Parallel plates	$\frac{V}{r}$	1.0
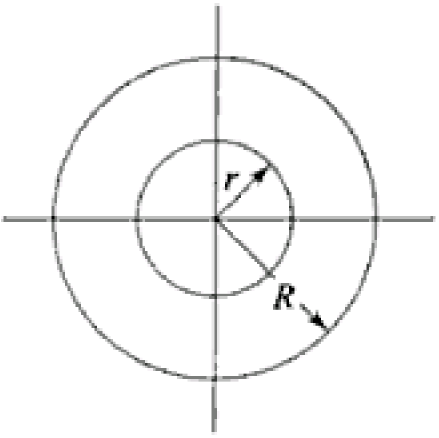 Concentric cylinders	$\frac{V}{r \ln \frac{R}{r}}$	$\frac{(R-r)}{r \ln \frac{R}{r}}$
Figure same as above Concentric spheres	$\frac{VR}{r\,(R-r)}$	$\frac{R}{r}$
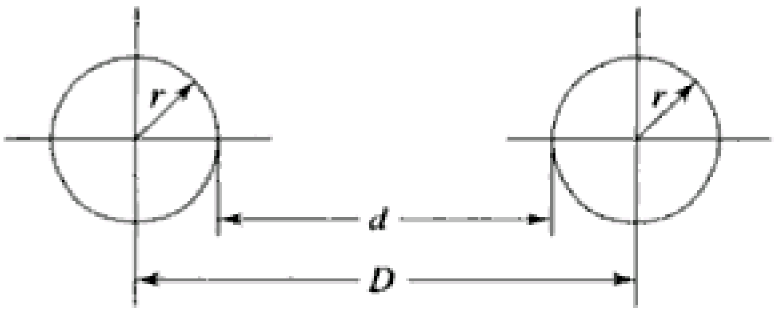 Parallel cylinders of equal diameter		$\frac{V\sqrt{D^2-4r^2}}{2r\,(D-r)\cosh^{-1}(D/2r)} \approx$ $\frac{V}{2r}\ln\frac{d}{r} \approx \frac{d}{2r\ln\frac{d}{r}}$ if $D \gg r$ (if $d \gg r$)
Equal spheres with dimensions as above	$\frac{V}{d}f$ $\approx \frac{V}{2r}$, if $d \gg r$	$f = \frac{\left(\frac{d}{r}+1\right)+\sqrt{\left(\frac{d}{r}+1\right)^2+8}}{4}$ $\approx \frac{d}{2r}$, if $d \gg r$

For other configurations like sphere-plane and cylinder-plane f is approximately given by

$$f = 0.94\,\frac{d}{r} = 0.8 \text{ (sphere-plane)}$$

$$f = 0.25\,\frac{d}{r} + 1.0 \text{ (cylinder-plane)}$$

Many electric conductors are normally either plane, cylindrical, or spherical in shape or can be approximated to these shapes. In other situations the conductors may be approximated into spheroidal, elliptical, toroidal and other geometrical shapes, and thus estimation of E_m can be made.

1.6 NUMERICAL METHODS FOR ELECTRIC FIELD COMPUTATION

1.6.1 Introduction

In recent years, several numerical methods for solving partial differential equations which include Laplace's and Poisson's equations have become available. There are inherent difficulties in solving these equations for two or three dimensional fields with complex boundary conditions, or for insulating materials with different permittivities and/or conductivities.

Proper design of any high voltage apparatus requires a complete knowledge of the electric field distribution. For a simple physical system with some symmetry, it is possible to find an analytical solution. However, in many cases, the physical systems are very complex and therefore in such cases, numerical methods are employed for the calculation of electric fields. Essentially, four types of numerical methods are commonly employed in high voltage engineering applications. They are: Finite Difference Method (FDM), Finite Element Method (FEM), Charge Simulation Method (CSM) and Surface Charge Simulation Method (SSM) or Boundary Element Method (BEM). The first two methods are generally classified as domain methods and the last two are categorized as boundary methods.

The principal task in the computation of electric field is to solve the Poisson's equation Eq. (1.10). In case of space charge-free fields the equation reduces to Laplace's equation Eq. (1.11). Personal computers have the required computational power to solve these problems. However, computing times and the amount of memory to achieve the desired accuracy still play a dominant role. Further, another important aspect for the acceptance of a method is the ease with which it can be used to describe the problem. A brief description of each of these methods is given in the following sections.

1.6.2 Finite Difference Method (FDM)

Apart from other numerical methods for solving partial differential equations, the Finite Difference Method (FDM) is universally applied to solve linear and even non-linear problems. Although the applicability of difference equations to solve the Laplace's equation was used earlier, it was not until 1940s that FDMs have been widely used. The applicability of FDMs to solve general partial differential equation is well documented in specialised books.

The field problem for which the Laplace's or Poisson's equation applies is given within a (say x, y), plane, the area of which is limited by given boundary conditions, i.e. by contours on which some field quantities are known. Every potential φ and its distribution within the area under consideration will be continuous. Therefore, an unlimited number of $\varphi(x, y)$ values will be necessary to describe the complete potential distribution. Since any numerical computation can provide only a limited amount of information, discretization of the area will be necessary to represent all the nodes for which the solution is needed. Such nodes are generally produced by any net or grid laid down on the area as shown in Fig. 1.2.

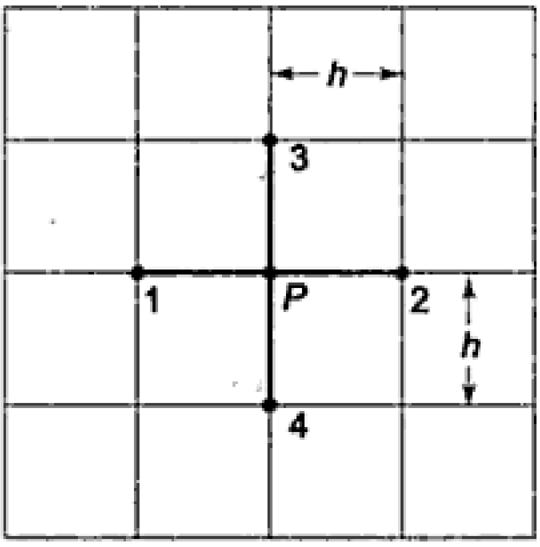

Fig. 1.2 *Illustrating the finite difference method*

The unknown potential φ (*p*) can be expressed by the surrounding potentials which are assumed to be known for the single difference equation. For every two-dimensional problem, most of the field region can be subdivided by a regular square net. Then, if the step size chosen for discretization is *h*, the following approximate equation becomes valid.

$$\varphi_1 + \varphi_2 + \varphi_3 + \varphi_4 - 4\varphi\,(p) + h^2 F(p) = 0 \qquad (1.13)$$

In the above equation, $\varphi_1 + \varphi_2 + \varphi_3 + \varphi_4$ are the potentials at the immediate neighbourhood nodes with respect to the node *p* of interest (of which the potential $\varphi(p)$ needs to be determined). The potentials at the neighbourhood points are expected to be known a priori, either from given boundary conditions or from any previous computational results. The term $F(p)$ arises if the field region is governed by the Poisson's equation, (i.e. the relation $\nabla^2\phi = F(p)$ holds good).

Thus, any general field problem to be treated needs sub-division of the finite plane by a predominantly regular grid, which is supplemented by irregular elements at the boundaries, if required. The whole grid will then contain *n* nodes, for which the potential $\varphi(p)$ is to be calculated. Then, a system of *n* simultaneous equations would result. Here, it may be noted that simple problems with small number of unknowns can be treated by long hand computation using the concept of residuals and point relaxation. For more complex problems, machine computation is necessary and iterative schemes are most efficient in combination with successive relaxation methods.

1.6.3 Finite Element Method (FEM)

Finite Element Method is widely used in the numerical solution of electric field problems, and became very popular. In contrast to other numerical methods, FEM is a very general method and therefore is a versatile tool for solving wide range of electric field problems.

The finite element analysis of any problem involves basically four steps:

(a) Finite Element Discretization

To start with, the whole problem domain is ficticiously divided into small areas/ volumes called *elements* (see Fig. 1.3). The potential, which is unknown throughout the problem domain, is approximated in each of these elements in terms of the potential at their vertices called *nodes*. As a result of this the potential function will be unknown only at the nodes. Normally, a certain class of polynomials, is used for the interpolation of the potential inside each element in terms of their nodal values. The coefficients of this interpolation function are then expressed in terms of the unknown nodal potentials. As a result of this, the interpolation can be directly carried out in terms of the nodal values. The associated algebraic functions are called *shape functions*. The elements derive their names through their shape, i.e. bar elements in one dimension (1D), triangular and quadrilateral elements in 2D, and tetrahedron and hexahedron elements for 3D problems.

(b) Governing Equations

The potential V_e within an element is first approximated and then interrelated to the potential distributions in various elements such that the potential is continuous across inter-element boundaries. The approximate solution for the whole region then becomes

$$V(x, y) = \sum_{e=1}^{N} V_e(x, y) \tag{1.14}$$

where N is the number of elements into which the solution region is divided.

The most common form of approximation for the voltage V within an element is a polynomial approximation

$$V_e(x, y) = a + bx + cy \tag{1.15}$$

For the triangular element, and for the quadrilateral element the equation becomes

$$V_e(x, y) = a + bx + cy + dxy \tag{1.16}$$

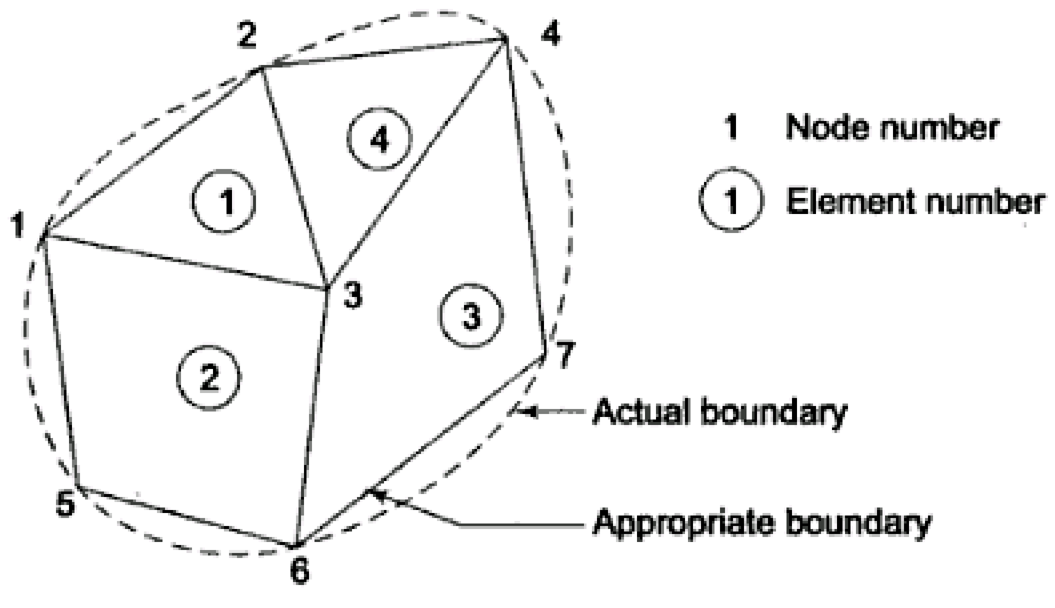

Fig. 1.3 *A typical finite element subdivision of an irregular domain*

The potential V_e in general is not zero within the element e but it is zero outside the element in view of the fact that the quadrilateral elements are non-confirming elements (see Fig. 1.3).

Consider a typical triangular element shown in Fig. 1.4. The potentials V_{e1}, V_{e2} and V_{e3} at nodes 1, 2, and 3 are obtained from Eq. (1.15), as

$$\begin{bmatrix} V_{e1} \\ V_{e2} \\ V_{e3} \end{bmatrix} = \begin{bmatrix} 1 & x_1 & y_1 \\ 1 & x_2 & y_2 \\ 1 & x_3 & y_3 \end{bmatrix} \begin{bmatrix} a \\ b \\ c \end{bmatrix} \tag{1.17}$$

the coefficients a, b, and c are determined from the above equation as

$$\begin{bmatrix} a \\ b \\ c \end{bmatrix} = \begin{bmatrix} 1 & x_1 & y_1 \\ 1 & x_2 & y_2 \\ 1 & x_3 & y_3 \end{bmatrix}^{-1} \begin{bmatrix} V_{e1} \\ V_{e2} \\ V_{e3} \end{bmatrix} \tag{1.18}$$

Substituting this equation in Eq. (1.15), we get

$$V_e = [1 \quad x \quad y] \frac{1}{2A}$$

$$\begin{bmatrix} (x_2y_3 - x_3y_2) & (x_3y_1 - x_1y_3) & (x_1y_2 - x_2y_1) \\ (y_2 - y_3) & (y_3 - y_1) & (y_1 - y_2) \\ (x_3 - x_2) & (x_1 - x_3) & (x_2 - x_1) \end{bmatrix} \begin{bmatrix} V_{e1} \\ V_{e2} \\ V_{e3} \end{bmatrix}$$

or,

$$V_e = \sum_{i=1}^{N} \alpha_i (x, y)\, V_{ei} \tag{1.19}$$

where,

$$\alpha_1 = (1/2\,A)\,[(x_2y_3 - x_3y_2) + (y_2 - y_3)x + (x_3 - x_2)y] \tag{1.20a}$$

$$\alpha_2 = (1/2\,A)\,[(x_3y_1 - x_1y_3) + (y_3 - y_1)x + (x_1 - x_3)y] \tag{1.20b}$$

$$\alpha_3 = (1/2\,A)\,[(x_1y_2 - x_2y_1) + (y_1 - y_2)x + (x_2 - x_1)y] \tag{1.20c}$$

and A is the area of the element e, that is,

$$2A = \begin{bmatrix} 1 & x_1 & y_1 \\ 1 & x_2 & y_2 \\ 1 & x_3 & y_3 \end{bmatrix}$$

$$= (x_1y_2 - x_2y_1) + (x_3y_1 - x_1y_3) + (x_2y_3 - x_3y_2)$$

or

$$A = 1/2\,[(x_2 - x_1)(y_3 - y_1) - (x_3 - x_1)(y_2 - y_1)] \tag{1.21}$$

The value of A is positive if the nodes are numbered counterclockwise (starting from any node) as shown by the arrow in Fig. 1.4. It may be noted that Eq. (1.19) gives the potential at any point (x, y) within the element provided that the potentials at the vertices are known. These are called the element shape functions. They have the following properties:

$$\alpha_1(x_1, y_1) = \begin{bmatrix} 1 \\ 0 \end{bmatrix} \begin{bmatrix} i = j \\ i \neq j \end{bmatrix} \tag{1.22a}$$

$$V_e = \sum_{i=1}^{3} \alpha_i (x, y) = 1 \tag{1.22b}$$

The energy per unit length associated with the element e is given by the following equation:

$$W_e = 1/2\ \varepsilon\ [V_e]^T\ [C^{(e)}]\ [V_e] \tag{1.23}$$

where, T denotes the transpose of the matrix

$$[V_e] = \begin{bmatrix} V_{e1} \\ V_{e2} \\ V_{e3} \end{bmatrix} \tag{1.24a}$$

and

$$[C^{(e)}] = \begin{bmatrix} C_{11}^{(e)} & C_{12}^{(e)} & C_{13}^{(e)} \\ C_{21}^{(e)} & C_{22}^{(e)} & C_{23}^{(e)} \\ C_{31}^{(e)} & C_{32}^{(e)} & C_{33}^{(e)} \end{bmatrix} \tag{1.24b}$$

The matrix given above is normally called as element coefficient matrix. The matrix element $C_{ij}^{(e)}$ of the coefficient matrix is considered as the coupling between nodes i and j.

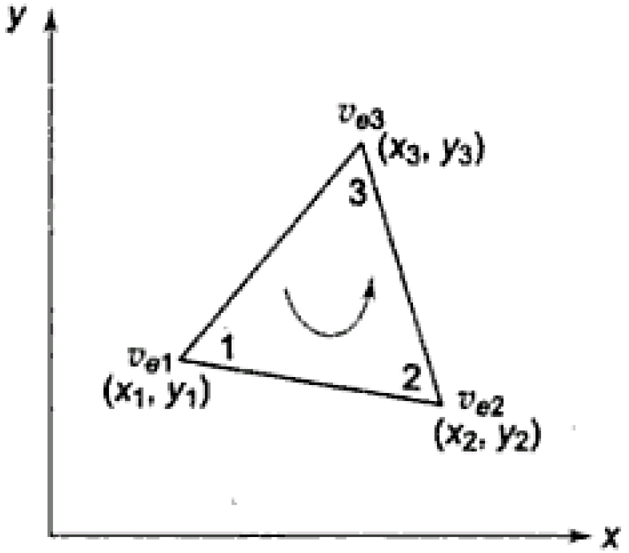

Fig. 1.4 *Typical triangular element; the local node numbering 1–2–3 must proceed counterclockwise as indicated by the arrow*

(c) Assembling of All Elements

Having considered a typical element, the next stage is to assemble all such elements in the solution region. The energy associated with all the elements will then be

$$W_e = \sum_{e=1}^{N} W_e = 1/2E\,[V]^T\,[C]\,[V] \tag{1.25}$$

where
$$[V] = \begin{bmatrix} V_1 \\ V_2 \\ \vdots \\ V_n \end{bmatrix} \tag{1.26}$$

and, n is the number of nodes, N is number of elements and $[C]$ is called the global coefficient matrix which is the sum of the individual coefficient matrices.

(d) Solving the Resulting Equations

It can be shown that the Laplace's (and Poisson's) equation is satisfied when the total energy in the solution region is minimum. Thus, we require that the partial derivatives of W with respect to each nodal value of the potential is zero, i.e.

$$\delta W/\delta V_1 = \delta W/\delta V_2 = \ldots\ \delta W/\delta V_n = 0$$

or,
$$\delta W/\delta V_k = 0 \text{ if } k = 1, 2, \ldots,\ n. \tag{1.27}$$

In general, $\delta W/\delta V_k = 0$ leads to

$$0 = \sum_{e=1}^{n} V_i C_{ik} \tag{1.28}$$

where, n is the number of nodes in the mesh. By writing the above Eq. (1.28) for all the nodes, $k = 1, 2, \ldots\ n$, we obtain a set of simultaneous equations from which the solution for $V_1, V_2 \ldots V_n$ can be found. This can be done either by using the Iteration Method or the Band Matrix Method.

Now, for solving the nodal unknowns, one cannot resort directly to the governing partial differential equations, as a piece-wise approximation has been made to the unknown potential. Therefore, alternative approaches have to be sought. One such classical approach is the *calculus of variation*. This approach is based on the fact that potential will distribute in the domain such that the associated energy will reach extreme values. Based on this approach, Euler has showed that the potential function that satisfies the above criteria will be the solution of corresponding governing equation. In FEM, with the approximated potential function, extremization of the energy function is sought with respect to each of the unknown nodal potential. This process leads to a set of linear algebraic equations. In this matrix form, these equations form normally a symmetric sparse matrix, which is then solved for the nodal potentials.

Within the individual elements the unknown potential function is approximated by the shape functions of lower order depending on the type of element. An approximate solution of the exact potential is then given in the form of an expression whose terms are the products of the shape function and the unknown nodal potentials. It can be shown that the solution of the differential equation describing the problem corresponds to minimization of the field energy. This leads to a system of algebraic equations the solution for which under the corresponding boundary conditions gives the required nodal potentials. Thus, this procedure results in a potential distribution in the form of discrete potential value at the nodal points of the FEM mesh. The related field strengths at the centres of all elements are then obtained from the potential gradient. The values of the field thus obtained are dependent on the distance between the centres of the elements and the electrode surface, and thus on the sizes of the elements.

1.6.4 Charge Simulation Method (CSM)

Charge Simulation Method (CSM) belongs to the family of integral methods for calculation of electric fields. There are two variations of this method: CSM with discrete charges and CSM with area charges.

CSM with discrete charges is based on the principle that the real surface charges on the surface of electrodes or dielectric interfaces are replaced by a system of point and line charges located outside the field domain. The position and the type of simulation charges are to be determined first and then the magnitudes of the charges are calculated so that their combined effect satisfies the boundary conditions. After determining these magnitudes by using the method of solving a system of liner equations, it is to be verified whether the systems of simulation charges fulfills the boundary conditions between the location points with sufficient accuracy. Then the voltage and field strength at any point within the field domain can be calculated analytically by the superposition of simple potential and gradient functions.

(a) Basic Principle of CSM

When the conductor is excited by an applied voltage, charges appear on the surface of the conductor. These charges produce an electric field outside the conductor, while at the same time maintains the conductor at equipotential. Similarly, when a dielectric is excited by an external field, it gets polarized, i.e. the charged particles of the molecules of the dielectric get shifted from their neutral state to produce a volume of dipoles. In essence, it is possible to replace this volume polarization by the charged surface. CSM employs this physical description and attempts to simulate the above-mentioned continuous charge distribution by a set of discrete charges kept just outside the computational domain. The values of these discrete charges are then evaluated by forcing the specified voltages at some selected points called *contour points* on the surface of the conductor and by forcing the material interface conditions at some selected points on the dielectric interface.

It is required that at any of these contour points on the electrode, the potential resulting from the superposition of the charges is equal to the electrode potential φ.

Thus

$$\varphi_i = \sum_{j=1}^{N} P_{ij}\, Q_j \tag{1.29}$$

where, P_{ij} are the potential coefficients which can be evaluated analytically for many types of charges by solving Laplace's or Poisson's equation. For example, in Fig. 1.5 which shows three point charges Q_1, Q_2 and Q_3 in free space, the potential φ_i at point C_i will be

$$\begin{aligned}\varphi_i &= Q_1/(4\pi\varepsilon_0 R_1) + Q_2/(4\pi\varepsilon_0 R_2) + Q_3/(4\pi\varepsilon_0 R_3)\\ &= P_{i1}Q_1 + P_{i2}Q_2 + P_{i3}Q_3\end{aligned} \tag{1.30}$$

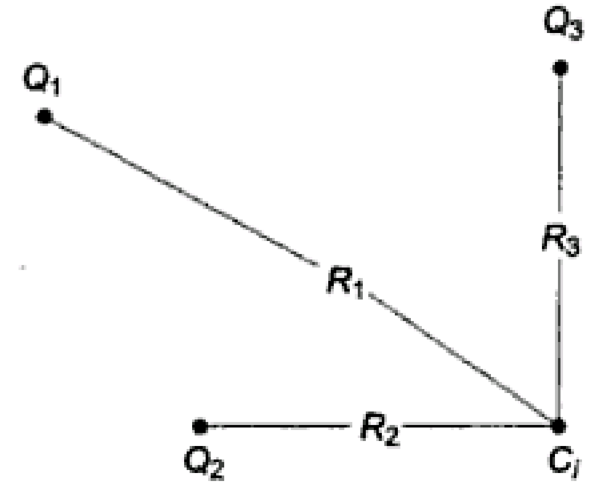

Fig. 1.5 *Three point charges in free space*

Thus, once the types of charges and their locations are defined, it is possible to relate φ_{ij} and Q_j quantitatively at any boundary point. In CSM, the simulation charges are placed outside the space where the field solution is desired (or inside any equipotential surface such as metal electrodes). If the boundary point C_i is located on the surface of a conductor, then φ_i at this contour point will be equal to the conductor potential φ. When this procedure is applied to m contour points, it leads to the following system of m linear equations for n unknown charges.

$$\begin{bmatrix} P_{11} & P_{12} & \cdots & P_{1n} \\ P_{21} & P_{22} & \cdots & P_{2n} \\ \vdots & \vdots & \vdots & \vdots \\ P_{m1} & P_{m2} & \cdots & P_{mn} \end{bmatrix} \begin{bmatrix} Q_1 \\ Q_2 \\ \vdots \\ Q_n \end{bmatrix} = \begin{bmatrix} \varphi_1 \\ \varphi_2 \\ \vdots \\ \varphi_m \end{bmatrix} \tag{1.31}$$

This equation is the basis of the CSM as discussed below.

(b) Use of CSM for a Single Dielectric Medium

If there are N conductors with known potentials in a single dielectric medium, then, for the calculation of field, the actual charges on the surfaces of these conductors are replaced by n_c fictitious charges placed inside or outside the conductors. The types and positions of these charges are assumed. In order to determine their magnitudes, n_b contour points are selected on the surfaces of the conductors, at known or fixed potentials and it is required that at any of these contour points the potential resulting from superposition of all the simulation charges is equal to the known conductor potential. The number of contour points is selected equal to the number of ficticious charges, i.e. $n_b = n_c = n$. Therefore, the charges are determined from

$$[P]_{n,n}\,[Q]_n = [\varphi]_n \tag{1.32}$$

where, $[P]$ = potential coefficient matrix, $[Q]$ = column vector of values of unknown charges, and $[\varphi]$ = potential of the boundary points.

After solving Eq. (1.32) to determine the magnitudes of simulation charges, it is necessary to check whether the set of calculated charges produces the actual boundary conditions everywhere on the electrode surfaces. It is possible that the potential at any point other than the contour points can be different from the actual conductor potential. Thus, Eq. (1.29) is solved at a number of *check points* located on the electrodes where potentials are known to determine the simulation accuracy. If simulation does not meet the accuracy criterion, calculations are repeated by changing either the number or the location or the types of simulation charges and the locations of contour points.

Once adequate charge system has been determined, the potential and field at any point outside the electrodes can also be calculated.

(c) CSM for a Multi-Dielectric Medium

The field computations for a multi-dielectric system are more complicated than for a single dielectric. This is due to the fact that, under the influence of applied voltage, the dipoles are re-aligned in a dielectric, and this re-alignment has the effect of producing a net surface charge on the dielectric. Thus, in addition to the electrodes, each dielectric-dielectric interface needs to be simulated by the discrete charges. In the simple example of Fig. 1.6, charges 1 to 3 are used to simulate the electrode while charges 4 to 7 are used to simulate the dielectric boundary. Contour points 1 to 3 are selected on the electrode surface whereas only two contour points (i.e. 4 and 5) are selected on the dielectric boundary. In order to determine the simulation charges, a system of equations is formulated by imposing the following boundary conditions:

- at each electrode boundary, potential must be equal to the known conductor potential, and
- at each dielectric boundary, potential and normal component of the flux density must be same, when viewed from either side of the boundary.

In formulating the equations at a given contour point, the charges which lie in the same dielectric as the contour point are ignored. For example, the potential at control point 1 is calculated by the superposition of charges 1 to 5. Similarly, the potential or field intensity at contour point 5 when viewed from the side of dielectric A will be due to the superposition of charges 1 to 3 and 6 and 7. Thus, when the first boundary condition is applied to contour points 1 to 3, (i.e. i, = 1 to 3) the following equations are obtained.

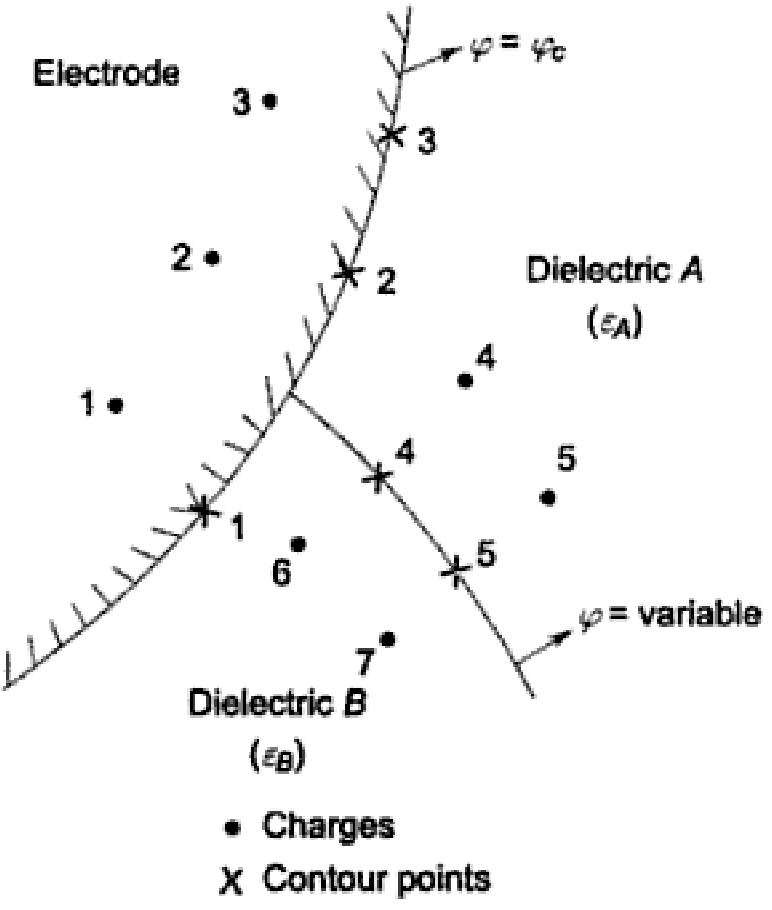

Fig. 1.6 *Simulation of multi-dielectric boundary*

$$\sum_{j=1}^{5} P_{ij}Q_j = \varphi_c \; (i = 1) \tag{1.33}$$

$$\sum_{j=1}^{3} P_{ij}Q_j + \sum_{j=6}^{7} P_{ij}Q_j = \varphi_c \quad (i = 2, 3) \tag{1.34}$$

When the second boundary condition is applied for potential and the flux density at $i = 4$ to 5, the following equations are obtained:

$$\sum_{j=4}^{5} P_{ij}Q_j + \sum_{j=6}^{7} P_{ij}Q_j = 0 \tag{1.35}$$

$$(\varepsilon_A - \varepsilon_B) \sum_{j=1}^{3} f_{ij}Q_j + \varepsilon_A \sum_{j=6}^{7} f_{ij}Q_j - \varepsilon_B \sum_{j=4}^{5} f_{ij}Q_j = 0 \tag{1.36}$$

for $i = 4, 5$, where, f_{ij} are the field coefficients in a direction which is normal to the dielectric boundary at the respective contour point. The above equations are solved to determine the unknown charges. The accuracy of simulation of multidielectric boundaries deteriorates when the dielectric boundary has a complex profile.

The error in the CSM depends upon the type, number as well as the locations of the simulation charges, the locations of contour points and the complexities of the profile of the electrodes and the dielectrics.

1.6.5 Boundary Element Method (BEM)

Though the charge simulation method is known for its accuracy and speed, it is not very efficient in case of multi-dielectric problems and very thin electrodes, which are often used to control and get the electric field strength in condenser bushings, transformers, etc. Such problems can be solved using the Surface Charge Simulation Method (SSM) which is also called Boundary Element Method (BEM).

In many cases, electrodes and insulators used in high voltage equipment consists of cylinders, spheres, cones, and plane electrodes. Therefore, it is necessary to consider elements having these shapes to achieve a realistic field simulation by using variable charge distribution on these surfaces. The elements are combined in computer code and used for the calculation of complex geometries wherever possible. Curved triangles are employed only at those positions where the above elements cannot be used. This method requires a large number of elements, normally more than 2000, independent of the surface shape and therefore leads to a very large number of system equations.

(a) Principle of BEM

BEM, in principle, is very similar to CSM with area elements. Like in CSM, the BEM uses area charge elements to replace the real charges. However, BEM does not require that the system components should have actual symmetry. The discretization of the real charges is generally carried out by boundary elements having three or four nodes, which use linear shape functions to approximate the internal charge distribution. If the outer surface geometry is not covered, then suitable intermediate points can be added. Boundary elements having predetermined shapes like cylinders, cones, spheres and toroids are available. The evaluation of the resulting potential functions of the boundary elements is done by numerical integration.

(b) Basic Formulation of BEM

Boundary element formulation calls for the scalar electric potential due to surface charge density, which is written as

$$\varphi(\xi) = 1/(2\alpha\pi\varepsilon_0) \int_{\gamma} \rho_s(x)\, \Phi^I(\xi, x)\, dP(x) \qquad (1.37)$$

where, φ^I denotes the fundamental solution of the potential problem, $\alpha = 1$ or 2 for two or three-dimensional problems respectively, and $\rho_s(x)$ denotes the surface charge density. Equation (1.37) is the basic equation for the source formulation of the BEM. This equation can be solved using the standard point collocation procedure for discretized image charges that lie within the conducted boundaries. The collocation approach has been recognized as charge simulation. The electric field is then given by.

$$\varphi(\xi) = 1/(2\alpha\pi\varepsilon_0) \int_{\gamma} \rho_s(x) \, \nabla\Phi^1 \, (\xi, x); \, dP(x) \tag{1.38}$$

The resulting system of equations obtained using the source formulation will again be asymmetric. By solving this system of equations, the unknown values of the charge density can be found. Once the charge distribution is known, potential and electric field values can be calculated throughout the domain using Eqs. (1.37) and (1.38) given above.

1.6.6 Relative Advantages and Disadvantages of the Various Numerical Methods

For computing the electric fields, various methods have been used, viz. Finite Difference Method, Finite Element Method, Charge Simulation Method and Boundary Element Method. Each of these methods has its own advantages for solving a particular problem.

With the FDM, the numerical evaluation of the difference equation is simple but time consuming. For treating a given field problem, it is necessary to subdivide the finite plane of the field problem into a predominantly regular net of polygons which is supplemented with irregular elements at the boundaries. However, in this method, all difference equations are approximation to the field equation by neglecting the higher order terms. Thus, the resulting error can be large.

On the other hand, Finite Element Method is a very general method and has been used for solving a variety of problems. Any non-linearity/inhomogeneity can be modelled and the solution will be available on the entire surface of the domain. Material interface conditions are automatically satisfied. However, it needs a powerful graphic user interface for processing.

Open geometry does not pose any problem with the Charge Simulation Method since the surface of the conductor is the only one that is discretized. In addition, as the solution satisfies the Laplace's/Poisson's equation, it will be very smooth, and always gives a small but dense matrix and therefore can be easily handled using personal computers. However, due to the application of superposition principle, non-linearities and non-homogeneity cannot be modelled using this method.

On the other hand a unique feature of Boundary Element Method is that the electric fields are proportional to the charge densities on an enclosed electrode which is simulated by real charges. This direct field derivation is based on a well known Gauss's area integral. Although BEM is sufficiently developed for use in two-dimensional axi-symmetric problems, some difficulties still exist. They are, the programming complexity and the need for large amount of computational time to execute an improper integral.

Of the above methods, the choice of a particular method depends on the specific problem on hand. In general, the construction of Finite Element model requires considerable effort, since the entire field region should be meshed, while the Charge Simulation and Boundary Element Methods require only the outer surface of the electrode and the outer layer of the dielectric to be meshed. In practice, an important difference between the various numerical methods is that the Finite Element Method can be used only with fields which are bounded while the Charge Simulation method and the Boundary Element Methods can also deal with unbounded fields.

A comparison of the accuracies of using the various computational methods shows a good agreement between the results of BEM and FEM, for two-dimensional problems a discrepancy is about 1% while in the 3-D case it is about 2%. On the other hand, descrepancies between BEM and FEM are 2% in the case of 2D calculations and 3% in the case of 3D problems.

For FEM applications, there are a few commercially available software packages like ANSYS (Ansoft Corporation Inc.) and NISA (Engineering Mechanics Research Centre). However, the electric field computations based on other methods like FDM, CSM and BEM generally require programmes to be developed individually by the user.

1.6.7 Conclusion

As described above, various numerical methods for the calculation of electric fields have already been established as reliable tools for high voltage engineers. However, efforts are still being continued to provide better accuracy and to solve more complicated problems. Now a days, the maximum number of unknowns available in various methods has remarkably increased with the availability of large computational capacity.

The various numerical methods have been described only briefly. For further study, two review papers (References 13 and 14) and more papers dealing with the principles and applications of these methods for field calculations are added in References 15–29.

1.7 SURGE VOLTAGES, THEIR DISTRIBUTION AND CONTROL

The design of power apparatus particularly at high voltages is governed by their transient behaviour. The transient high voltages or surge voltages originate in power systems due to lightning and switching operations. The effect of the surge voltages is severe in all power apparatuses. The response of a power apparatus to the impulse or surge voltage depends on the capacitances between the coils of windings and between the different phase windings of the multi-phase machines. The transient voltage distribution in the windings as a whole are generally very non-uniform and are complicated by travelling wave voltage oscillations set up within the windings. In the actual design of an apparatus, it is, of course, necessary to consider the maximum voltage differences occurring, in each region, at any instant of time after the application of an impulse, and to take into account their durations especially when they are less than one microsecond.

An experimental assessment of the dielectric strength of insulation against the power frequency voltages and surge voltages, on samples of basic materials, on less complex assemblies, or on complete equipment must involve high voltage testing. Since the design of an electrical apparatus is based on the dielectric strength, the design cannot be completely relied upon, unless experimentally tested. High voltage testing is done by generating the voltages and measuring them in a laboratory.

When high voltage testing is done on component parts, elaborate insulation assemblies, and complete full-scale prototype apparatus (called development testing), it is possible to build up a considerable stock of design information; although expensive, such data can be very useful. However, such data can never really be complete to cover all future designs and necessitates use of large factors of safety. A different approach to the problem is the exact calculation of dielectric strength of any insulation arrangement. In an ideal design each part of the dielectric would be uniformly stressed at the maximum value which it will safely withstand. Such an ideal condition is impossible to achieve in practice, for dielectrics of different electrical strengths, due to the practical limitations of construction. Nevertheless it provides information on stress concentration factors—the ratios of maximum local voltage gradients to the mean value in the adjacent regions of relatively uniform stress. A survey of typical power apparatus designs suggests that factors ranging from 2 to 5 can occur in practice; when this factor is high, considerable quantities of insulation must be used. Generally, improvements can be effected in the following ways:

(i) by shaping the conductors to reduce stress concentrations,
(ii) by insertion of higher dielectric strength insulation at high stress points, and
(iii) by selection of materials of appropriate permittivities to obtain more uniform voltage gradients.

The properties of different insulating media and their applications are presented in Chapters 2, 3, 4 and 5. The generation and measurement of high voltages and currents are discussed in Chapters 6 and 7, and high voltage test methods and the design of high voltage laboratories are detailed in Chapters 9, 10 and 11. The various aspects of insulation co-ordination in high voltage power systems are discussed in Chapter 8.

Key Terms

- Electric Field Stresses
- Insulators: Gases and Vacuum, Liquids, Solids and Composites
- Estimation of Electric Field
- Numerical Computation of Electric Field
- FEM
- CSM and BEM
- Field enhancement factor
- Surge voltage distribution and control

Multiple Choice Questions

1. Average electrical field is the magnitude of electrical field
   - (a) at mid point between conductors
   - (b) ratio of potential difference to the distance between the conductors
   - (c) at surface of the lower potential electrode
   - (d) ratio of potential difference to half the distance between the conductors.
2. An experimental method for computing the field distribution is
   - (a) solution of Laplace equation
   - (b) electrolytic tank method
   - (c) digital simulation
   - (d) field intensity method.
3. Field enhancement factor is the ratio of
   - (a) maximum field to average field
   - (b) rms value of electric field to average value
   - (c) potential difference to radius of the conductor
   - (d) electric field at surface of the h.v. conductor to electric field at ground conductor.
4. A numerical method to determine electric field in a multi-conductor geometry is
   - (a) electrolytic tank method
   - (b) resistance analog method
   - (c) finite element method
   - (d) Laplace equation method.
5. Most suitable numerical method to solve electrostatic field problems is
   - (a) Laplace equation method
   - (b) charge simulation method
   - (c) finite difference method
   - (d) resistance analog method.
6. Open geometry does not pose any problem with
   - (a) boundary element method
   - (b) charge simulation method
   - (c) finite difference method
   - (d) resistance analog method.
7. A unique feature of the Boundary Element Method is that
   - (a) it can be used for electric fields which are uniform only
   - (b) it can be used only with bounded fields
   - (c) electric field are proportional to the charge densities on an enclosed electrode which is simulated by real charges
   - (d) none of the above.
8. Finite Element Method can be used only with
   - (a) fields which are bounded
   - (b) fields which are unbounded
   - (c) fields which are both bounded and unbounded
   - (d) when high accuracy is not required.
9. A comparison of the accuracies of various computational methods shows a good agreement between the results of
   - (a) FEM and FDM
   - (b) FDM and BEM
   - (c) FEM and CSM
   - (d) BEM and FEM.

Answers

1. (b)
2. (b)
3. (a)
4. (c)
5. (b)
6. (b)
7. (c)
8. (a)
9. (d)

Review Questions

1.1 What are the different dielectric materials according to their physical nature?
1.2 How is the Electric Stress/Electric Field Intensity controlled?
1.3 Define field factor. How does it vary in simple geometries?
1.4 Discuss the different numerical methods available for estimation of electric field distribution in dielectric media.
1.5 What is "Finite Element method"? Give the outline of this method for solving the field problems.
1.6 Discuss briefly the "Charge Simulation Method" for solving Field Problems and estimation of potential distribution.
1.7 What is "Boundary Element Method"? How does it differ from Charge Simulation Method?
1.8 Discuss the relative advantages and disadvantages of different numerical methods for solution of field problems.

References

1. Alston, L.L., *High Voltage Technology*, Oxford University Press, Oxford (1967).
2. Seely, S., *Electromagnetic Fields*, McGraw-Hill, New York (1960).
3. Kuffel E., Zaengl, W.S. and Kuffel, J., *High Voltage Engineering Fundamentals*, (2nd edition), Butterworths Heinemann (2000).
4. Popovic, B.D., *Introductory Engineering Electromagnetics*, Addison-Wesley (1971).
5. Chari, M.V.K. and Silvester, P.P., *Finite Elements in Electrical and Magnetic Field Problems*, Wiley-Interscience Publication, John Wiley and Sons, New York (1980).
6. Silvester, P.P., and Ferrari, R.L., *Finite Elements for Electrical Engineers*, Cambridge University Press (1983).
7. Binns, K.J. and Lawrenson, P.J., *Analysis and Computation of Electric and Magnetic Field Problems*, (2nd edition), Pergamon Press (1973).

Contd.

8. Zienkiewicz, O.C., *The Finite Element Method in Engineering Science*, McGraw-Hill, London (1977).
9. Anderson, O.W., "Finite Element Solution of Complex Potential Electric Fields". *IEEE Transaction on power apparatus and systems*, **97**, 1156–1166 (1977).
10. Singer, H., Steinbirglar, H. and Weiss, P., "A Charge Simulation Method for the Calculation of H.V. Fields", *IEEE Transactions on PAS,* **93** 1660–1668, (1974).
11. Malik, N.H., "A review of Charge Simulation Method and its Applications", *IEEE Transactions on Electrical Insulation,* **EI-24** No. 13–20 (1989).
12. Brebbia, C.A., Telles, J.C.F., and Wrobel, L.C., *Boundary Element Techniques*, Springer-Verlag, (1984).
13. Takuma, T., "Recent developments in calculation of electric and magnetic fields related to high voltage engineering", *Key Note Speech, Proc. of 12th Int. Symp. on High Voltage Engineering*, Bangalore, India (20–24 August 2001).
14. Takuma, T., Kawamoto, T., "Recent developments in electric field calculation", *IEEE Trans. on Magnetics*, **33**, No. 2, pp. 1155–1160 (1997).
15. Singer, H., "Computation of optimized electrode geometries", 3rd, *Int. Symp. on High Voltage Engineering (ISH), Paper No. 11.06* (1979).
16. Trinitis, C., "Field optimization of three dimensional high voltage equipment", *11th ISH, London, Paper No. 2.75.* P6 (1999).
17. Anderson, O.W., "Finite element solution for complex potential electric fields", *IEEE Trans. on Power Apparatus and systems*, **86**, pp 1156–1161 (1977).
18. Ryan, H.M., "Electric Field of a Rod-Plane Spark gap", *IEE Proceedings*, 117, pp 283 (1970).
19. Abou Seada, M.S., and Nasser, E., "Digitial Computer Calculation of the Electric Potential and Field of a Rod gap", *IEEE Proceedings.* **56**, pp 813–818 (1988).
20. Anderson, O.W., "Laplacian Electrostatic field calculation by Finite elements with automatic grid generation", *IEEE Trans. On Power Apparatus and Systems,* **PAS-92**, No. 5, pp 1485–1493 (1973).
21. Miri, A.M., Riegel, N.A., Kuhner, A., "Finite Element Models for the Computation of the Transient Potential and Field Distribution in the Winding System of High Voltage Power Transformers," *11th ISH, London, Paper No. 2.39.S4* (1999).

Contd.

22. Iravani, M.R., and Raghuveer, M.R., "Accurate field solution in the entire interelectrode space of a rod-plane gap using optimized charge simulation", *IEEE Trans. Electrical Insulation*, 17, No. 4, pp 333–337 (1982).
23. Yializis, Kuffel, E., Alexander, P.N., "An optimized Charge Simulation Method for the calculation of High Voltage Fields", *IEEE Trans. on Power Apparatus and Systems*, **PAS-97**, pp 2434–2440 (1978).
24. Steinbigler, H., "Combined application of Finite Element Method and Charge Simulation Method for the computation of Electric fields", *3rd International Symposium on High Voltage Engineering, Milan, Paper No. 11.11.* August, 1979.
25. Malik, N.H., and Al-Arainy, A., "Charge simulation modeling of three-core belted cables", *IEEE Trans. Electrical Insulation,* **20**, No. 3, pp 499–503 (1985).
26. Kato, S., "An Estimation method for the Electric Field error of Charge Simulation Method", *3rd International Symposium on High Voltage Engineering, Milan, Paper No. 11.09.* August 1979.
27. Gutfleish, F., Singer, H., Forger, K. and Gomollon, J.A., "Calculations of HV Fields by means of the Boundary Element Method", *IEEE Transactions on PWRD* **9**, pp 734-749 (1994).
28. Chakravorti, S., and Mukherjee, P.K., "Power frequency and impulse field calculation around an HV insulator with uniform and non-uniform surface pollution", *IEEE Trans.* on *Electrical Insulation, EI-28,* pp. 43–53 (1993).
29. de Kock, N., Mendik, M., Andjelic, Z., Blaszcyzk, and A., "Application of the 3D Boundary Element Method in the Design of EHV GIS Components", *IEEE Elec. Ins. Mag.*, **14**, No. 3, pp. 17–22 (1998).

2

Conduction and Breakdown in Gases

2.1 | GASES AS INSULATING MEDIA

The simplest and the most commonly found dielectrics are gases. Most of the electrical apparatus use air as the insulating medium, and in a few cases other gases such as nitrogen (N_2), carbon dioxide (CO_2), freon (CCl_2F_2) and sulphur hexafluoride (SF_6) are also used.

Various phenomena occur in gaseous dielectrics when a voltage is applied. When the applied voltage is low, small currents flow between the electrodes and the insulation retains its electrical properties. On the other hand, if the applied voltages are large, the current flowing through the insulation increases very sharply, and an electrical breakdown occurs. A strongly conducting spark formed during breakdown practically produces a short circuit between the electrodes. The maximum voltage applied to the insulation at the moment of breakdown is called the breakdown voltage. In order to understand the breakdown phenomenon in gases, a study of the electrical properties of gases and the processes by which high currents are produced in gases is essential.

The electrical discharges in gases are of two types, i.e. (i) non-sustaining discharges, and (ii) self-sustaining types. The breakdown in a gas, called spark breakdown is the transition of a non-sustaining discharge into a self-sustaining discharge. The build-up of high currents in a breakdown is due to the process known as ionization in which electrons and ions are created from neutral atoms or molecules, and their migration to the anode and cathode respectively leads to high currents. At present two types of theories, viz. (i) Townsend theory, and (ii) Streamer theory are known which explain the mechanism for breakdown under different conditions. The various physical conditions of gases, namely, pressure, temperature, electrode field configuration, nature of electrode surfaces, and the availability of initial conducting particles are known to govern the ionization processes.

2.2 | COLLISION PROCESSES

2.2.1 Types of Collision

An electrical discharge is normally created from unionised gas by collision processes. These processes are mainly gas processes which occur due to the collision between the charged particles and gas atoms or molecules. These are of the following two types.

Elastic collisions: Elastic collisions are collisions which when occur, no change takes place in the internal energy of the particles but only their kinetic energy gets redistributed. These collisions do not occur in practice. When electrons collide with gas molecules, a single electron traces a zig-zag path during its travel. But in between the collisions it is accelerated by the electric field. Since electrons are very light in weight, they transfer only a part of their kinetic energy to the much heavier ions or gas molecules with which they collide. This results in very little loss of energy by the electrons and therefore electrons gain very high energies and travel at a much higher speed than the ions. Therefore in all electrical discharges electrons play a leading role.

Inelastic collisions: Inelastic collisions, on the other hand, are those in which internal changes in energy take place within an atom or a molecule at the expense of the total kinetic energy of the colliding particle. The collision often results in a change in the structure of the atom. Thus all collisions that occur in practice are inelastic collisions. For example ionisation, attachment, excitation, recombination are inelastic collisions.

2.2.2 Mobility of Ions and Electrons

When an ion moves through a gas under the influence of a static uniform electric field, it gains energy from the field between collisions and loses energy during collisions. Electric force on an electron/ion of charge e is eE, with the resulting acceleration being eE/m. When the energy gained by the ions from the electric field is small compared with the thermal energy, the drift velocity in the field direction W_i is proportional to the electrical field intensity E and may be expressed as follows:

$$W_i = \mu_i E \tag{2.1}$$

where μ_i is called the mobility of ions. The mobility is mainly a characteristic of the gas through which the ion moves. At normal temperatures and pressures the mobility μ is of the order of several cm^2/volt-sec.

However, the concept of ionic mobility cannot be directly applied to electrons because of their extremely low mass. Any externally applied electric field will

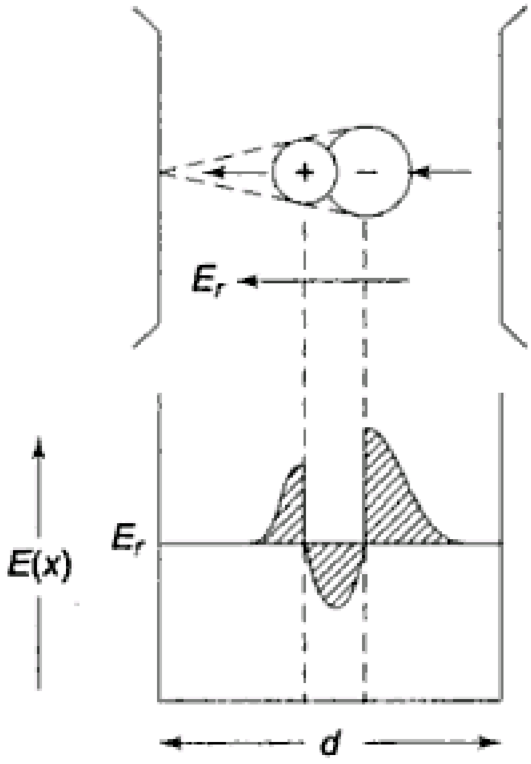

Fig. 2.11 *Field distortion in a gap due to space charge*

Further, cloud chamber photographs of the avalanche development have shown that, under certain conditions, the space charge developed in an avalanche can transform the avalanche into streamers which lead to very rapid development of breakdown.

In the theories proposed by Raether and Meek it has been shown that when the avalanche in the gap reaches a critical size, the combined applied field and the space charge field cause intense ionization and excitation of the gas particles in front of the avalanche. Instantaneous recombination between positive ions and electrons releases photons which in turn produce secondary electrons by photo-ionization. These secondary electrons under the influence of the field in the gap develop into secondary avalanches as shown in Fig. 2.12. Since photons travel with the velocity of light, the photo-ionization process gives rise to rapid development of conduction channels across the gap.

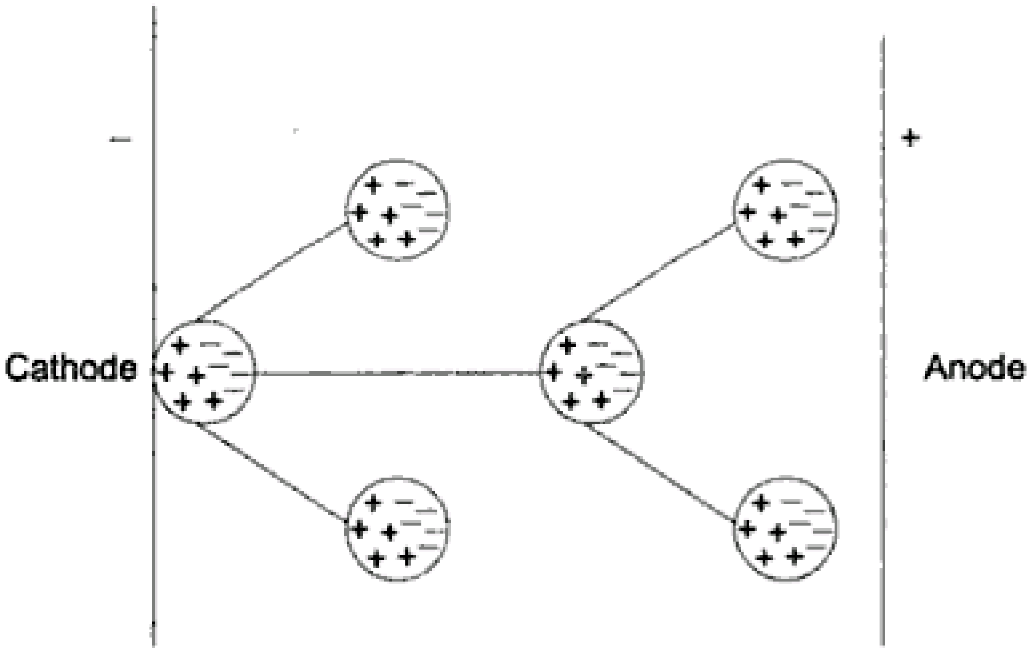

Fig. 2.12 *Formation of secondary avalanches due to photo-ionization*

On the basis of experimental observations Raether proposed an empirical expression for the streamer spark criterion of the form

$$\alpha x_c = 17.7 + \ln x_c + \ln (E_r/E) \tag{2.28}$$

where E_r is the space charged field directed radially at the head of the avalanche and E is the applied field.

The conditions for the transition from the avalanche to streamer assumes that the space charged field, E, approaches the externally applied field ($E = E_r$) and hence the breakdown criterion (Eq. (2.28)) becomes

$$\alpha x_c = 17.7 + \ln x_c \tag{2.29}$$

The minimum breakdown value for a uniform field gap by streamer mechanism is then obtained on the assumption that the transition from an avalanche to a streamer occurs when the avalanche has just crossed a gap, d. Thus, a minimum breakdown voltage by streamer mechanism occurs only when a critical length $x_c = d$.

Meek proposed a simple quantitative criterion to estimate the electric field that transforms an avalanche into a streamer. The field E_r produced by the space charge, at the radius r, is given by

$$E_r = 5.27 \times 10^{-7} \frac{\alpha \exp(\alpha x)}{(x/p)^{1/2}} \text{ V/cm} \tag{2.30}$$

where α is Townsend's first ionization coefficient, p is the gas pressure in torr, and x is the distance to which the streamer has extended in the gap. According to Meek, the minimum breakdown voltage is obtained when $E_r = E$ and $x = d$ in the above equation.

The equation simplifies into,

$$\alpha d + \ln\left(\frac{\alpha}{p}\right) = 14.5 + \ln\left(\frac{E}{p}\right) + \frac{1}{2}\ln\left(\frac{d}{p}\right) \tag{2.31}$$

This equation is solved between α/p and E/p at which a given p and d satisfy the equation. The breakdown voltage is given by the corresponding product of E and d.

The above simple criterion enabled an agreement between the calculated and the measured breakdown voltages. This theory also neatly fits in with the observed filamentary, crooked channels and the branching of the spark channels, and cleared up many ambiguities of the Townsend mechanism when applied to breakdown in a high pressure gas across a long gap.

It is still controversial as to which mechanism operates in uniform field conditions over a given range of pd values. It is generally assumed that for pd values below 1000 torr-cm and gas pressures varying from 0.01 to 300 torr, the Townsend mechanism operates, while at higher pressures and pd values the Streamer mechanism plays the dominant role in explaining the breakdown phenomena.

2.11 | PASCHEN'S LAW

It has been shown earlier (refer Sec. 2.6) that the breakdown criterion in gases is given as

$$\gamma[\exp(\alpha d) - 1] = 1 \tag{2.32}$$

where the coefficients α and γ are functions of E/p, i.e

$$\frac{\alpha}{p} = f_1\left(\frac{E}{p}\right)$$

and

$$\gamma = f_2\left(\frac{E}{p}\right)$$

Also

$$E = \frac{V}{d}$$

Substituting for E in the expressions for α and γ and rewriting Eq. (2.26) we have

$$f_2\left(\frac{V}{pd}\right)[\exp\left\{pdf_1\left(\frac{V}{pd}\right)\right\} - 1] = 1 \tag{2.33}$$

This equation shows a relationship between V and pd, and implies that the breakdown voltage varies as the product pd varies. Knowing the nature of functions f_1 and f_2 we can rewrite Eq. (2.32) as,

$$V = f(pd) \tag{2.34}$$

This equation is known as Paschen's law.

The Paschen's curve, the relationship between V and pd is shown in Fig. 2.13. It is seen that the relationship between V and pd is not linear and has a minimum value for any gas.

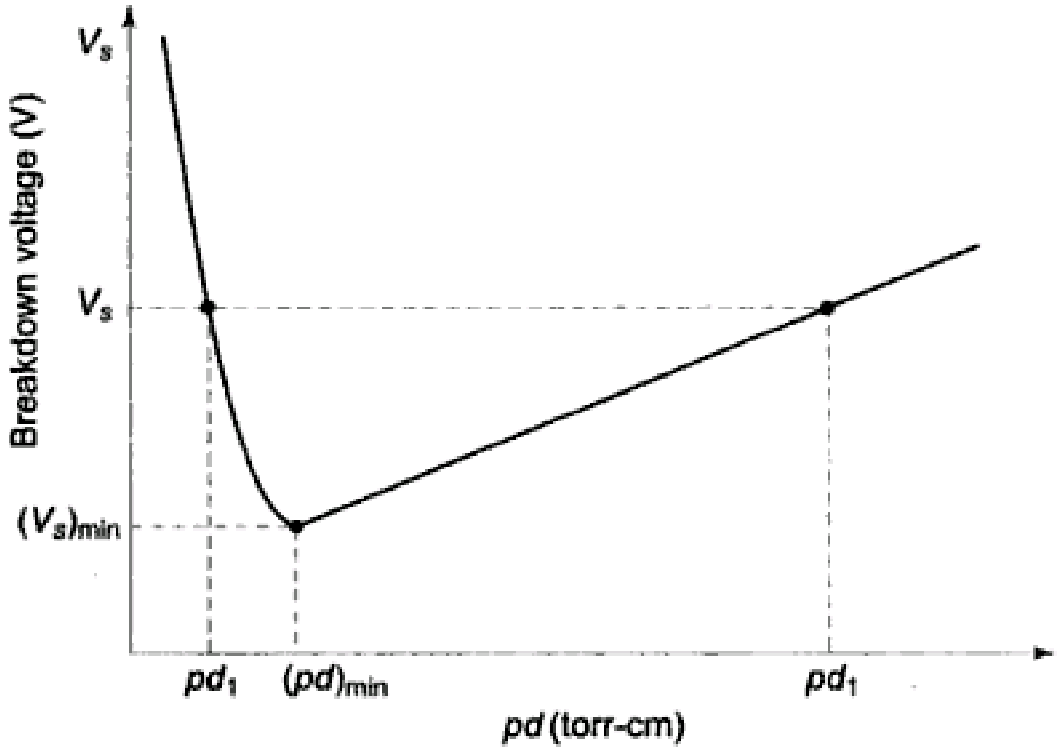

Fig. 2.13 *Breakdown voltage-pd curve (Paschen's law)*

This means that a breakdown voltage of a uniform field gap is a unique function of the product of p, the gas pressure and d, the electrode gap, for a particular gas and for a given electrode material.

Paschen's Law is found to be valid over a wide range of pd values as shown in Fig. 2.14. As can be seen from the figure, at higher pd values, the breakdown voltage in some gases is found to be slightly higher than the values at smaller gaps for the same values of pd. This departure from Paschen's law is probably due to the transition from the Townsend breakdown mechanism to the Streamer mechanism. On the other hand, at very low pressures, deviations from the Paschen's law are observed when the breakdown mechanism is not influenced by the properties of the gas but depends on the purity and property of the electrodes.

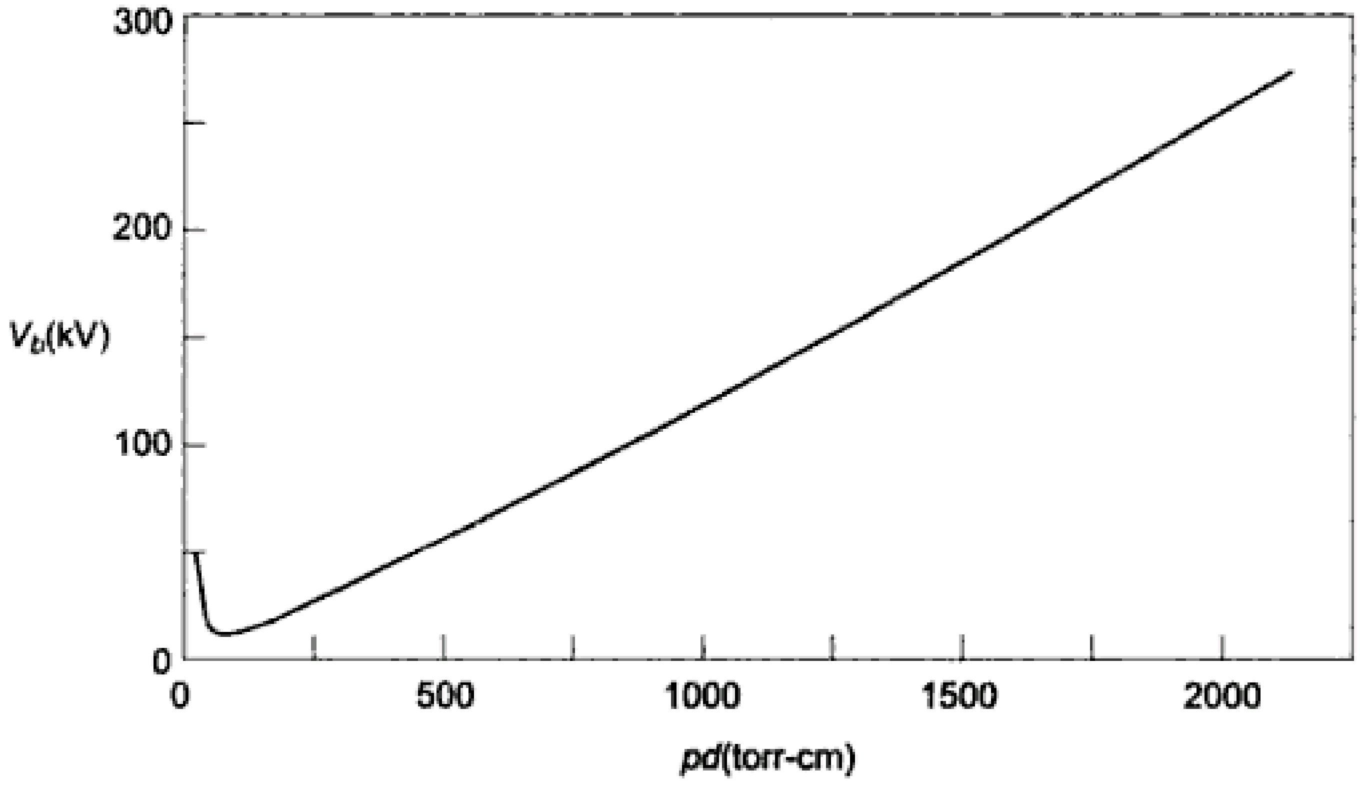

Fig. 2.14 *Breakdown voltage (V_b) as a function of pd in SF6. (Electrical Breakdown of Gases, edited by J.M. Meek and J.D.Craggs, John Wiley, New York, 1978)*

In order to account for the effect of temperature, the Paschen's law is generally stated as $V = f(Nd)$, where N is the density of the gas molecules. This is necessary, because the pressure of the gas changes with temperature according to the gas law pv = NRT, where v is the volume of the gas, T is the temperature, and R is a constant.

Based on the experimental results, the breakdown potential of air is expressed as a power function in pd as

$$V = 24.22\left[\frac{293\,pd}{760\,T}\right] + 6.08\left[\frac{293\,pd}{760\,T}\right]^{1/2} \tag{2.35}$$

It may be noted from the above formula that the breakdown voltage at constant pressure and temperature is not constant.

At 760 torr and 293 K.

$$E = V/d = 24.22 + \left[\frac{6.08}{\sqrt{d}}\right] \text{ kV/cm} \tag{2.36}$$

This equation yields a limiting value for E of 24 kV/cm for long gaps and a value of 30 kV/cm for $\left(\frac{293\,pd}{760\,T}\right) = 1$, which means a pressure of 760 torr at 20°C with 1 cm gap. This is the usually quoted breakdown strength of air at room temperature and at atmospheric pressure.

2.12 BREAKDOWN IN NON-UNIFORM FIELDS AND CORONA DISCHARGES

2.12.1 Corona Discharges

If the electric field is uniform, a gradual increase in voltage across a gap produces a breakdown of the gap in the form of a spark without any preliminary discharges. On the other hand, if the field is non-uniform, an increase in voltage will first cause a discharge in the gas to appear at points with highest electric field intensity, namely at sharp points or where the electrodes are curved or on transmission lines. This form of discharge is called a corona discharge and can be observed as a bluish luminescence. This phenomenon is always accompanied by a hissing noise, and the air surrounding the corona region becomes converted into ozone. Corona is responsible for considerable loss of power from high voltage transmission lines, and it leads to the deterioration of insulation due to the combined action of the bombardment of ions and of the chemical compounds formed during discharges. Corona also gives rise to radio interference.

The voltage gradient required to produce visual a.c. corona in air at a conductor surface, called the corona inception field, can be approximately given for the case of parallel wires of radius r as

$$E_w = 30\,md\left[1+\frac{0.301}{\sqrt{dr}}\right] \tag{2.37}$$

For the case of coaxial cylinders, whose inner cylinder has a radius r the equation becomes

$$E_c = 31\,md\left[1+\frac{0.308}{\sqrt{dr}}\right] \tag{2.38}$$

where m is the surface irregularity factor which becomes equal to unity for highly polished smooth wires; d is the relative air density correction factor given by,

$$d = \frac{0.392b}{(273+t)} \tag{2.39}$$

where b is the atmospheric pressure in torr, and t is the temperature in °C, $d = 1$ at 760 torr and 25°C. The expressions were found to hold good from atmospheric pressure down to a pressure of several torr.

On the high voltage conductors at high pressures there is a distinct difference in the visual appearance of the corona under positive and negative polarities of the applied voltage. When the voltage is positive, corona appears as a uniform bluish white sheath over the entire surface of the conductor. On the other hand, when the voltage is negative, the corona will appear like reddish glowing spots distributed along the length of the wire. Investigations with point-plane gaps in air showed that when point is negative, corona appears as current pulses called Trichel pulses, and the repetition frequency of these pulses increases as the applied voltage is increased and decreases with decrease in pressure. On the other hand, observations when the point is positive in air showed that the corona current increases steadily with voltage. At sufficiently high voltage, current amplification increases rapidly with voltage, up to a current of about 10^{-7} A, after which the current becomes pulsed with repetition frequency of about 1 kHz composed of small bursts. This form of corona is called burst corona. The average current then increases steadily with applied voltage leading to breakdown.

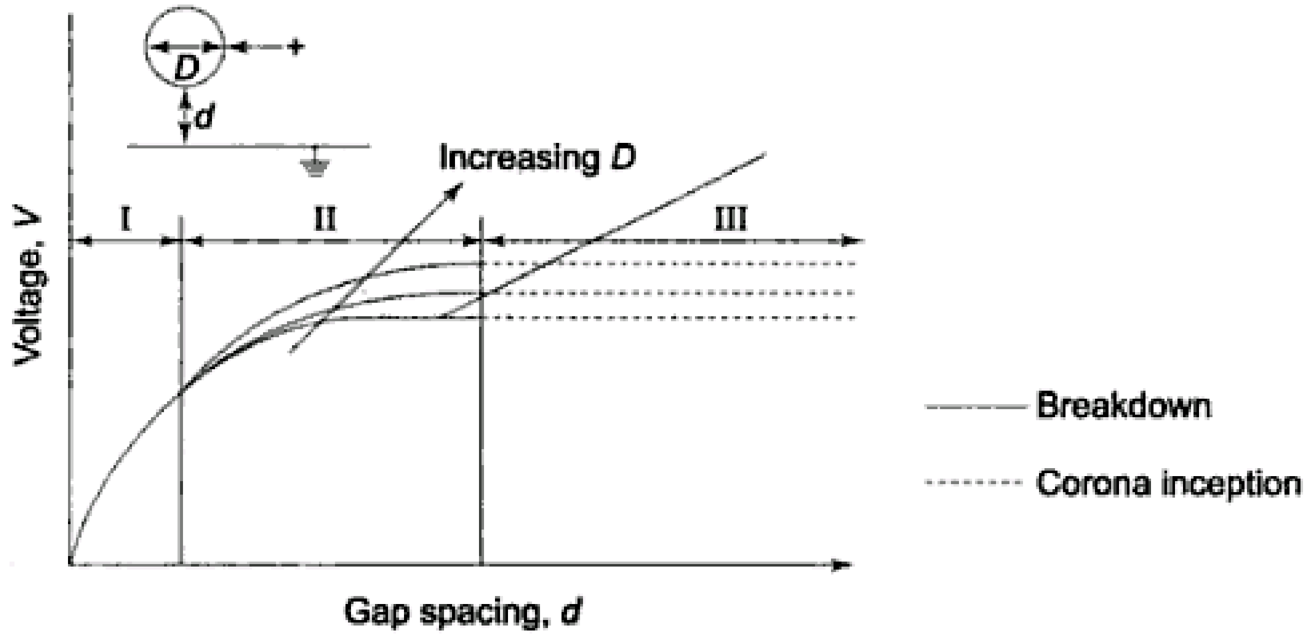

Fig. 2.15 *Breakdown and corona inception characteristics for spheres of different diameters in sphere-plane gap geometry*

The corona inception and breakdown voltages of the sphere-plane arrangement are shown in Fig. 2.15. From this figure it can be seen that

(a) at small spacings (region I), the field is uniform, and the breakdown voltage mainly depends on the spacing;
(b) at fairly large spacings (region II), the field is non-uniform, and the breakdown voltage depends both on the sphere diameter and the spacing; and
(c) at large spacings (region III), the field is non-uniform, and the breakdown is preceded by corona and is controlled only by the spacing. The corona inception voltage mainly depends on the sphere diameter.

It may be summarized that the study of corona and non-uniform field breakdown is very complicated and investigations are still under progress.

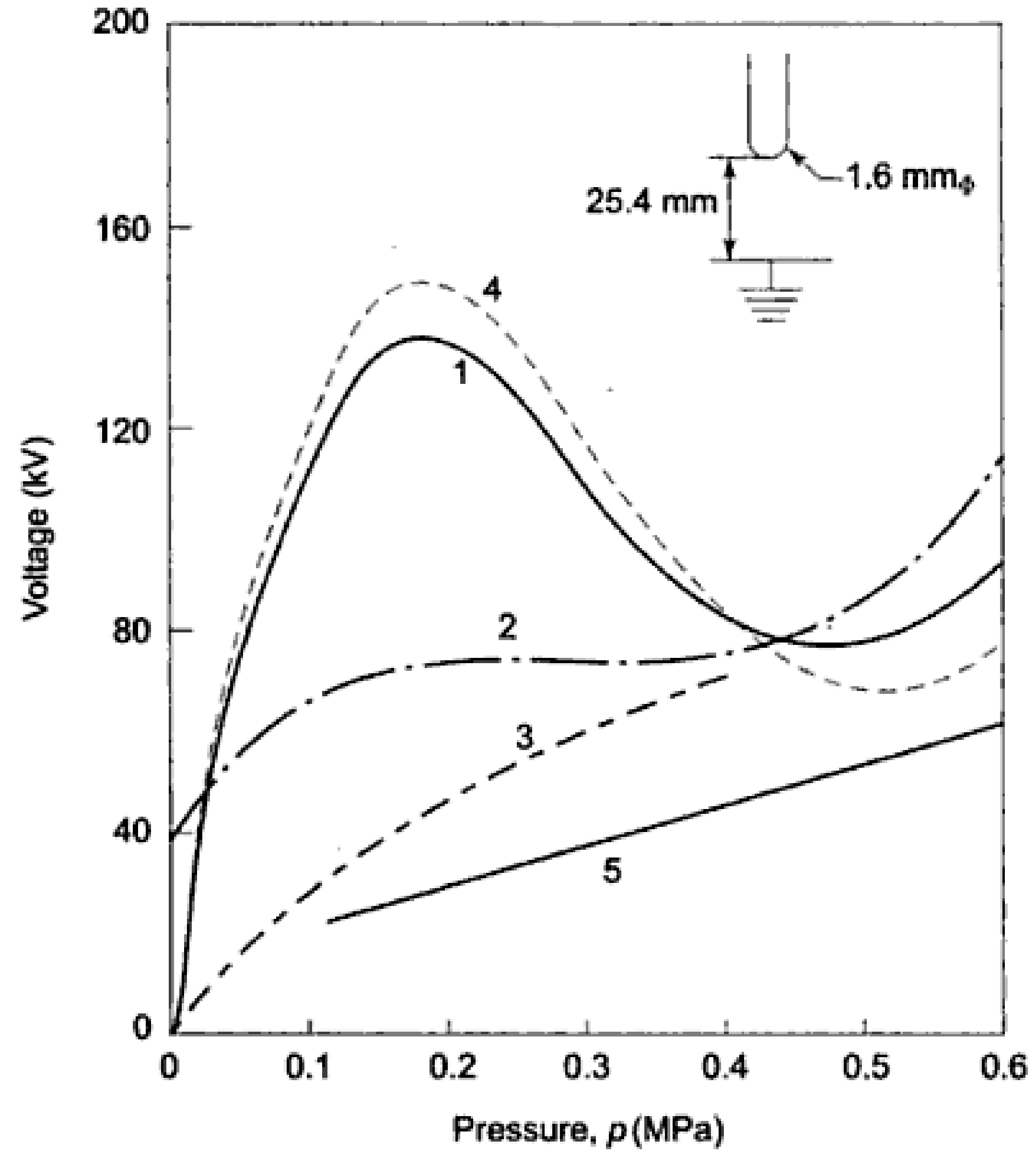

Fig. 2.16 *Breakdown characteristics of SF_6 and N_2 as a function of pressure*
1. SF_6 positive d.c. breakdown *2. SF_6 positive impulse breakdown*
3. SF_6 positive d.c. corona *4. SF_6 50 Hz a.c. breakdown*
5. SF_6 50 Hz a.c. corona

2.12.2 Breakdown in Non-uniform Fields

In non-uniform fields, such as coaxial cylinders, point-plane and sphere-plane gaps, the applied field varies across the gap. Similarly, Townsend's first ionization coefficient (α) also varies with the gap. Hence αd in Townsend's criterion [refer to Eq. (2.22)] is rewritten by replacing αd by $\int_0^d \alpha\, dx$. Townsend's criterion for breakdown now becomes

$$\gamma\left\{\exp\left[\int_0^d \alpha\, dx\right]-1\right\} = 1 \tag{2.40}$$

Meek and Raether also discussed the non-uniform field breakdown process as applied to their Streamer theory, and the Meek's equation [Eq. (2.27)] for the radial field at the head of an avalanche when it has crossed a distance x is modified as

$$E_r = \frac{5.27\times10^{-7}\,\alpha_x \exp\left(\int_0^x \alpha\,dx\right)}{(x/p)^{1/2}}\ \text{V/cm} \qquad (2.41$$

where α_x is the value of α at the head of the avalanche, and p is the gas pressure The criterion for the formation of the streamer is reached when the space charg field E_r approaches a value equal to the applied field at the head of the avalanche

This equation has been successfully used for determining the corona onse voltages of many non-uniform geometries. However, the condition for th advancement of streamers has not been arrived at so far. Figures 2.16 to 2.1 show the breakdown characteristics for SF_6 and SF_6/N_2 mixtures.

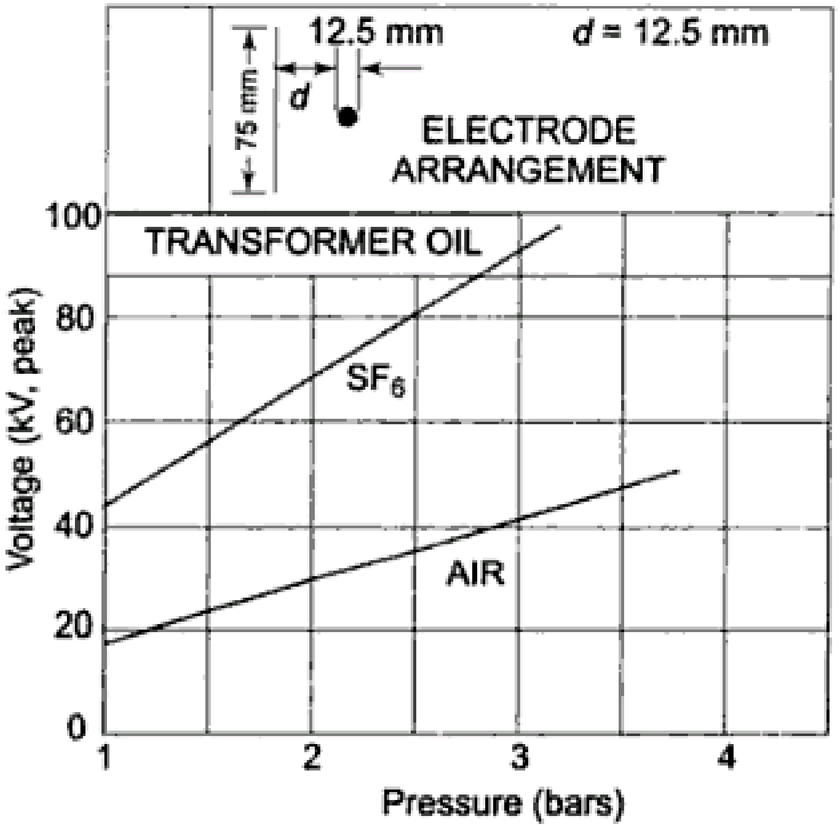

Fig. 2.17 *Breakdown voltage as a function of pressure in SF_6*

From the practical engineering point of view, rod-rod gap and sphere-sphere gap are of great importance, as they are used for the measurement of high voltages and for the protection of electrical apparatus such as transformers. The breakdown characteristics of rod-rod gaps are shown in Fig. 2.19. From this figure it can be seen that the breakdown voltages are higher for negative polarity The breakdown voltages were also observed to depend on humidity in air. In the case of rod gaps the field is non-uniform, while in the case of sphere gaps field is uniform, if the gap is small compared with the diameter. In the case of sphere gaps, the breakdown voltages do not depend on humidity and are also independent of the voltage waveform. The formative time lag is quite small (~ 0.5 μs) even with 5% over-voltage. Hence sphere gaps are used for breakdown voltage (peak value) measurements. These are further discussed in Chapter 7 (Sec. 7.2.6).

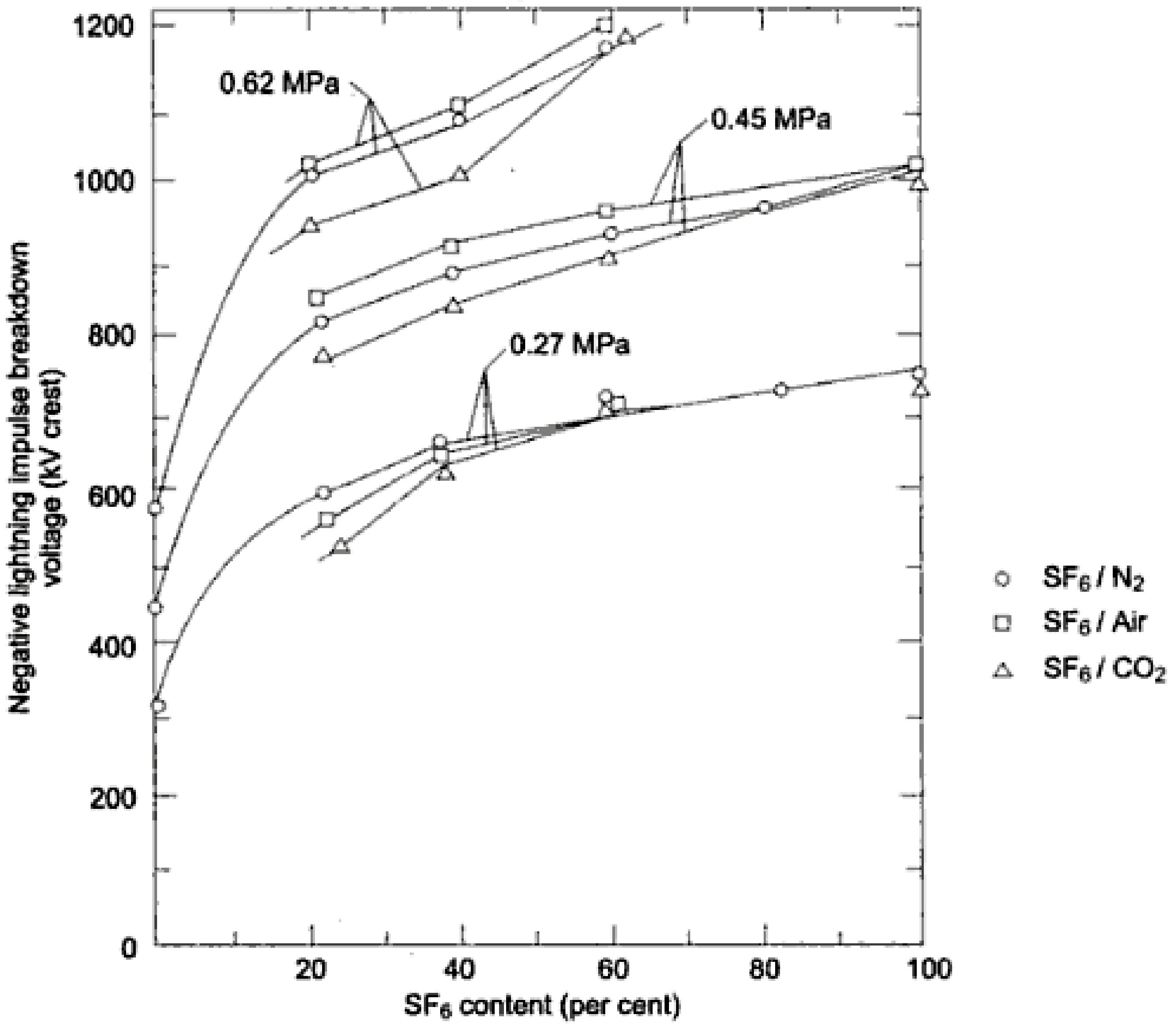

Fig. 2.18 *Negative lightning impulse (1.2/40 μs) breakdown Voltage in mixtures of SF_6 with N_2, Air and CO_2 for coaxial electrode system*

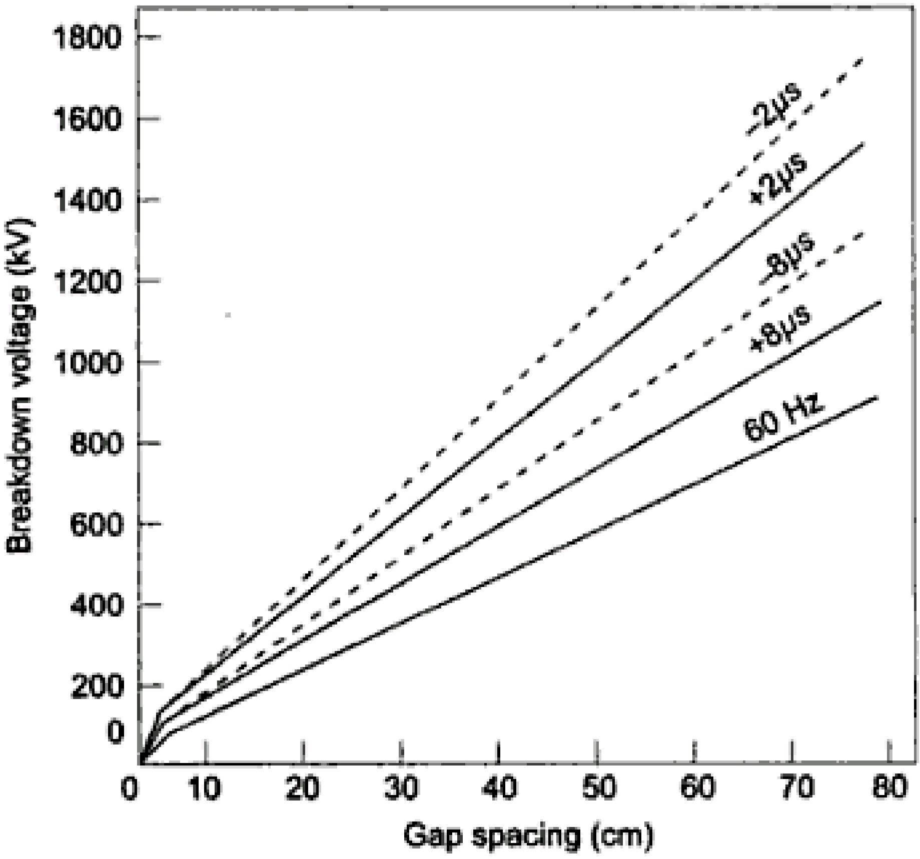

Fig. 2.19 *Power frequency (60 Hz) and impulse breakdown voltage curves for a rod-rod gap in air at n.t.p. One rod is earthed. Absolute humidity is 6.5 gms/ft^3. Impulse breakdown curves are for various times of breakdown on the wave tail.*
***ref.:** B.S.S. 171: 1959, power transformers*

2.13 | POST-BREAKDOWN PHENOMENA AND APPLICATIONS

This is the phenomenon which occurs after the actual breakdown has taken place and is of technical importance. Glow and arc discharges are the post-breakdown phenomena, and there are many devices that operate over these regions. In a Townsend discharge (see Fig. 2.20) the current increases gradually as a function of the applied voltage. Further to this point (B) only the current increases, and the discharge changes from the Townsend type to Glow type (BC). Further increase in current results in a very small reduction in voltage across the gap (CD) corresponding to the normal glow region. The gap voltage again increases (DE), when the current is increased more, but eventually leads to a considerable drop in the applied voltage. This is the region of the arc discharge (EG). The phenomena that occur in the region CG are the post-breakdown phenomena consisting of glow discharge (CE) and the arc discharge (EG).

Glow Discharge

A glow discharge is characterized by a diffused luminous glow. The colour of the glow discharge depends on the cathode material and the gas used. The glow discharge covers the cathode partly and the space between the cathode, and the anode will have intermediate dark and bright regions. This is called normal glow. If the current in the normal glow is increased such that the discharge covers the entire cathode surface, then it becomes abnormal glow. In a glow discharge, the voltage drop between the electrodes is substantially constant, ranging from 75 to 300 V over a current range of 1 mA to 100 mA depending on the type of the gas. The properties of the glow discharge are used in many practical applications, such as cold cathode gaseous voltage stabilized tubes (voltage regulation tubes or VR tubes), for rectification, as a relaxation oscillator, and as an amplifier.

Arc Discharge

If the current in the gap is increased to about 1 A or more, the voltage across the gap suddenly reduces to a few volts (20–50 V). The discharge becomes very luminous and noisy (region EG in Fig. 2.20). This phase is called the arc discharge and the current density over the cathode region increases to very high values of 10^3 to 10^7 A/cm^2. Arcing is associated with high temperatures, ranging from 1000°C to several thousand degrees celsius. The discharge will contain a very high density of electrons and positive ions, called the arc plasma. The study of arcs is important in circuit breakers and other switch contacts. It is a convenient high temperature high intensity light source. It is used for welding and cutting of metals. It is the light source in lamps such as carbon arc lamp. High temperature plasmas are used for generation of electricity through magneto-hydro dynamic (MHD) or nuclear fusion processes.

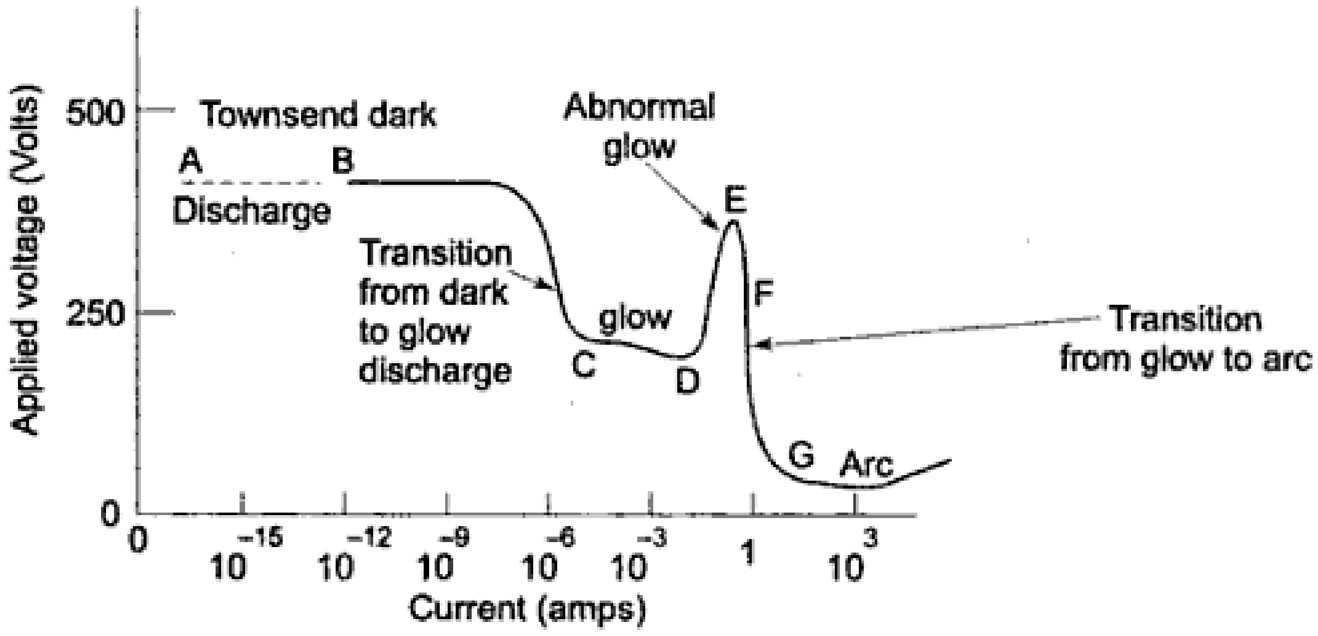

Fig. 2.20 *d.c. voltage-current characteristic of an electrical discharge with electrodes having no sharp points or edges*

2.14 PRACTICAL CONSIDERATIONS IN USING GASES AND GAS MIXTURES FOR INSULATION PURPOSES

Over the years, considerable amount of work has been done to adopt a specific gas for practical use. Before adopting a particular gas or gas mixture for a practical purpose, it is useful to gain a knowledge of what the gas does, what its composition is, and what the factors are that influence its performance. The greater the versatility of the operating performance demanded from an insulating gas or gas mixture, the more rigorous would be the requirements which it should meet. These requirements needed by a good dielectric do not exist in a majority of the gases. Generally, the preferred properties of a gaseous dielectric for high voltage applications are:

(a) high dielectric strength,
(b) thermal stability and chemical inactivity towards materials of construction,
(c) non-flammability and physiological inertness, and environmentally non-hazardous,
(d) low temperature of condensation,
(e) good heat transfer, and
(f) ready availability at moderate cost.

Sulphur hexafluoride (SF_6) which has received much study over the years has been found to possess most of the above requirements.

Of the above properties, dielectric strength is the most important property of a gaseous dielectric for practical use. The dielectric strength of gases is comparable with those of solid and liquid dielectrics (see Fig. 2.21).

It is clear that SF_6 has high dielectric strength and low liquefaction temperature, and it can be used over a wide range of operating conditions. SF_6 was also found to have excellent arc-quenching properties. Therefore, it is widely used as an insulating as well as arc-quenching medium in high voltage apparatus such as high voltage cables, current and voltage transformers, circuit-breakers and metal enclosed substations.

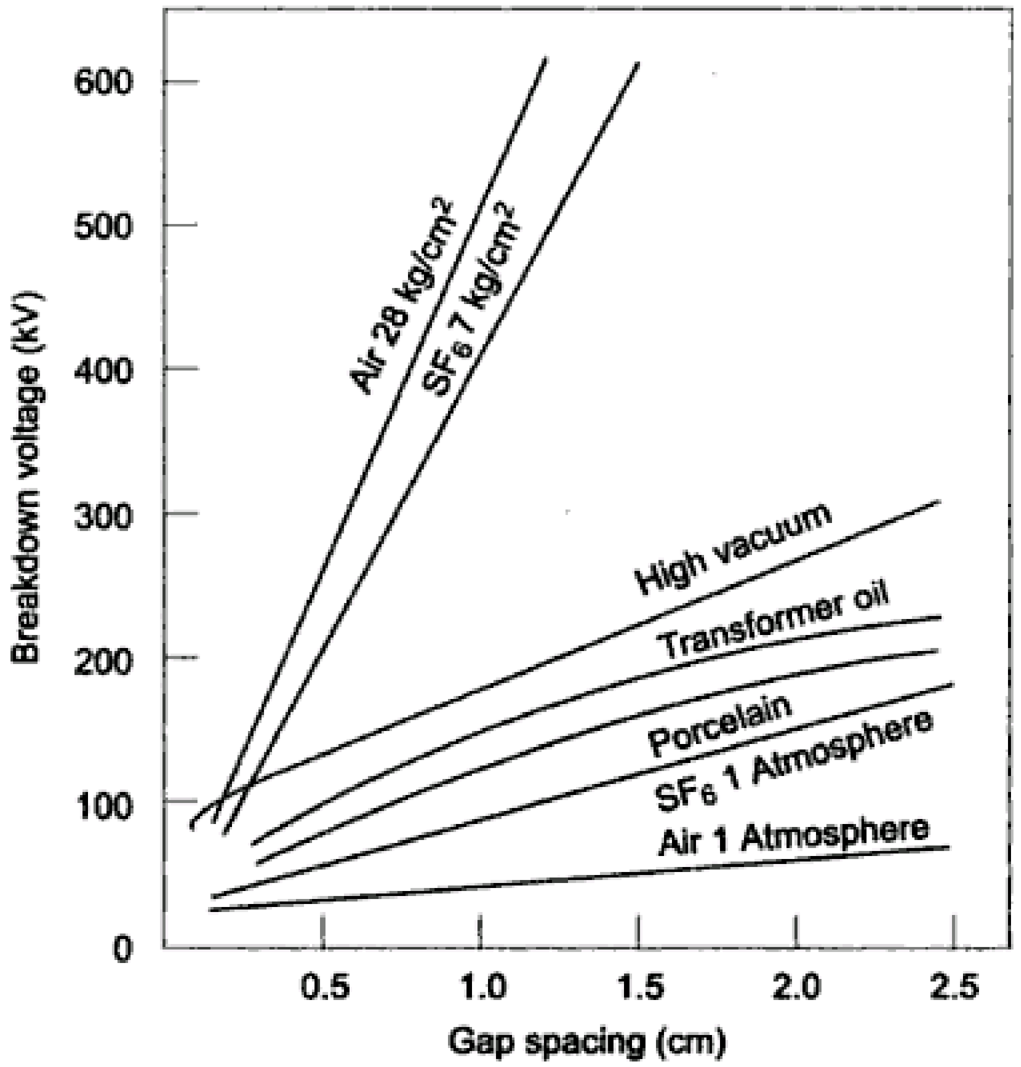

Fig. 2.21 *d.c. breakdown strength of typical solid, liquid, gas and vacuum insulations in uniform fields*

SF_6 and Other Gas Mixtures

SF_6 is widely used for applications in power system due to its high dielectric strength and good arc interruption properties. However, SF_6 gas has been found to be a green house gas that causes environmental problems. The production and use of SF_6 gas has increased steadily and today it is about 10,000 metric tons due to leakages into the atmosphere from the electrical equipment. The concentration of SF_6 in the environment has been steadily increasing. The release of SF_6 into the atmosphere leads to concentration of large volumes of SF_6 gas in the upper atmosphere. SF_6 molecules absorb energy from the sun and radiate it into the atmosphere for long duration of time.

There has been a large concern for these environmental effects and therefore the electrical industry has been looking for an alternate gas or gas mixture to be used in electrical equipment which presently use SF_6 gas, as an insulating and arc interruption medium. The large amount of experimental data that is presently available suggest that 40% SF_6/60% N_2 mixtures have all the dielectric characteristics that make it suitable for use as insulation in high voltage equipment. Ideally the gas mixture should be suitable for use in the existing equipment as well as in the equipment that will be designed and manufactured in future.

Extensive research work done in SF_6 and its mixtures with N_2, air and CO_2 has given breakdown values which are 80–90% of the pure SF_6 values as shown in Table 2.1.

Table 2.1 *Lightning Impulse Breakdown Strength of SF_6/Other Gas Mixtures*

Mixture Ratio	*Breakdown Strength (kV/cm)*
100% SF_6 gas	89.0
1% SF_6/99% Nitrogen	80.0
10% SF_6/90% Nitrogen	78.0
20% SF_6/80% Nitrogen	76.5
40% SF_6/60% Nitrogen	75.6
10% SF_6/90% CO_2	76.5
20% SF_6/80% CO_2	76.5
40% SF_6/60% CO_2	75.5
10% SF_6/90% Air	77.0
20% SF_6/80% Air	76.5
40% SF_6/60% Air	75.6

The industry is looking for a gas mixture that can replace the pure SF_6 gas in the existing SF_6 insulated apparatus, requiring no change in hardware, test procedures or ratings. SF_6/N_2 mixture is the one that has been found to be a good replacement for SF_6. SF_6/N_2 mixtures have been used in Gas Insulated Transmission System and were found to perform well. Also, the work done so far has shown that the ability of SF_6/N_2 mixtures to quench high current arcs is promising. The cost of such mixtures is low and are less sensitive to field non-uniformities present inside the equipment. In view of the above, the industry is trying to find out the optimum mixture ratio and the total pressure of the SF_6/N_2 mixture that would be required for a variety of applications. For many applications, such as Gas Insulated Transmission Systems, cables, capacitors, current transformers and voltage transformers, mixtures with different SF_6 concentrations varying from 5% to 40%.

SF_6/N_2 mixtures show promise as a medium in circuit breakers. It has been found that a mixture containing 69% SF_6/31% N_2 gave higher recovery rate than pure SF_6 at the same partial pressure. It has also been shown that it is possible to further improve the arc interruption properties of SF_6 by using SF_6/N_2 or SF_6/He mixtures.

In summary, it may be said that there is an urgent need to significantly reduce the use of SF_6 gas and its leakage from power apparatus. Use of gas mixtures appears to be feasible, but it has to be ensured that there is no loss in the performance of the equipment. Therefore, further research has to be carried out to identify a suitable gas mixture, its pressure and its arc interruption capability to be used in the existing apparatus and the apparatus that will be designed and manufactured in future.

2.15 | VACUUM INSULATION

2.15.1 Introduction

The idea of using vacuum for insulation purposes is very old. According to the Townsend theory, the growth of current in a gap depends on the drift of the charged particles. In the absence of any such particles, as in the case of perfect vacuum, there should be no conduction and the vacuum should be a perfect insulating medium. However, in practice, the presence of metallic electrodes and insulating surfaces within the vacuum complicate the issue and, therefore, even in vacuum, a sufficiently high voltage will cause a breakdown.

In recent years a considerable amount of work has been done to determine the electrical properties of high vacuum. This is mainly aimed at adopting such a medium for a wide range of applications in devices such as vacuum contactors and interrupters, high frequency capacitors and relays, electrostatic generators, microwave tubes, etc. The contactors and circuit breakers using vacuum as insulation are finding increasing applications in power systems.

2.15.2 What is Vacuum?

A vacuum system which is used to create vacuum is a system in which the pressure is maintained at a value much below the atmospheric pressure. In vacuum systems the pressure is always measured in terms of millimetres of mercury, where one standard atmosphere is equal to 760 millimetres of mercury at a temperature of 0°C. The term "millimetres of mercury" has been standardised as "Torr" by the International Vacuum Society, where one millimetre of mercury is taken as equal to one Torr. Vacuum may be classified as

High vacuum	:	1×10^{-3} to 1×10^{-6} Torr
Very high vacuum	:	1×10^{-6} to 1×10^{-8} Torr
Ultra high vacuum	:	1×10^{-9} torr and below.

For electrical insulation purposes, the range of vacuum generally used is the "high vacuum", in the pressure range of 10^{-3} Torr to 10^{-6} Torr.

2.15.3 Electron Emission in Vacuum

When the voltage across a small vacuum gap (< 2 mm) is increased, a relatively small current, mainly due to electrons, flows. For higher gaps (< 10 mm) small pulses of current, called microdischarges flow either independently or superposed over the steady current. For both the types of gaps subsequent increase of applied voltage causes the breakdown of the gap.

Several mechanisms have been proposed to explain electron emission from metallic surfaces. The most widely accepted mechanism is the cold emission model originally proposed by Fowler and Nordheim. Accordingly to this, the current density *J* due to field emission from sharp points on the electrode is given as:

$$J = AE^2 \exp[(-B\varphi 1.5\ v(y))/E]\ A/m^2 \qquad (2.42)$$

where $A = (1.54 \times 10^{-2})/[\varphi t^2(y)]$, $B = -6.831 \times 10^9$ and φ = work function of the metal.

The expression $t(y)$ and $v(y)$ are slow varying functions which are regarded as constants. The above equation therefore can be expressed as:

$$\log [J/E^2] = -\log [1/A]\ (-B\varphi^{1.5}\ v(y)\ (1/E))/2.3026 \qquad (2.43)$$

Since A, Φ and essentially $v(y)$ are constants, a plot of log J/E^2 against the reciprocal of E produces a straight line having a negative slope. This straight line is often used to assess the applicability of Fowler-Nordheim relation of the experimental data. However, in the case of electrodes with large area, the protrusions and uneven surfaces become unknown geometry. Therefore, to take account of these factors, Alpert modified the above equation as follows

$$\log [I/V^2] = -\log [1/(A'A\beta^2)]\ (-B\varphi^{1.5}\ v(y)\ [d/V]/2.3026\beta \qquad (2.44)$$

where A' is the electrode area and d is the gap length, J has been replaced by $(1/A')$, and the modified field is written as a product of local field enhancement factor β and the average field E (= V/d). The actual emitting area is replaced as $A'\beta^2$. Eqs. (2.42 to 2.44) have been experimentally confirmed by many investigators. If β is high and critical macroscopic field exceeds the field in the gap, the emitting site will explode releasing metal vapour.

In vacuum, electrode surfaces in long gaps produce low power pulses called microdischarges. These discharges have durations of 0.1 to 100 ms, frequency of 0.1 to 100 Hz and amplitudes of ≤ 10 mA. They may be caused by small particles of electrode material that are pulled out from one electrode and strike the other, or the beam of electrons from a cathode that can vapourize a small quantity of electrode material. At a given pressure, the frequency of occurrence of microdischarges increase with increase in applied voltage, eventually leading to breakdown.

2.15.4 Vacuum Breakdown

In the Townsend type of discharge in a gas described earlier, electrons get multiplied due to various ionization processes and an electron avalanche is formed. In a high vacuum, even if the electrodes are separated by, say, a few centimetres, an electron crosses the gap without encountering any collisions. Therefore, the current growth prior to breakdown cannot be due to the formation of electron avalanches. However, if a gas is liberated in the vacuum gap, then, breakdown can occur in the manner described by the Townsend process. Thus, the various breakdown mechanisms in high vacuum aim at establishing the way in which the liberation of gas can be brought about in a vacuum gap.

During the last 70 years or so, many different mechanisms for breakdown in vacuum have been proposed. These can be broadly divided into three categories

(a) Particle exchange mechanism
(b) Field emission mechanism
(c) Clump theory

(a) Particle Exchange Mechanism

In this mechanism it is assumed that a charged particle would be emitted from one electrode under the action of the high electric field, and when it impinges on the other electrode, it liberates oppositely charged particles due to ionization of adsorbed gases. These particles are accelerated by the applied voltage back to the first electrode where they release more of the original type of particles. When this process becomes cumulative, a chain reaction occurs which leads to the breakdown of the gap.

The particle-exchange mechanism involves electrons, positive ions, photons and the absorbed gases at the electrode surfaces. Qualitatively, an electron present in the vacuum gap is accelerated towards the anode, and on impact releases A positive ions and C photons. These positive ions are accelerated towards the cathode, and on impact each positive ion liberates B electrons and each photon liberates D electrons. This is shown schematically in Fig. 2.22. The breakdown will occur if the coefficients of production of secondary electrons exceeds unity. Mathematically, the condition for breakdown can be written as

$$(AB + CD) > 1 \tag{2.45}$$

Later, Trump and Van de Graaff measured these coefficients and showed that they were too small for this process to take place. Accordingly, this theory was modified to allow for the presence of negative ions and the criterion for breakdown then becomes

$$(AB + EF) > 1 \tag{2.46}$$

where A and B are the same as before and E and F represent the coefficients for negative and positive ion liberation by positive and negative ions. It was experimentally found that the values of the product EF were close enough to unity for copper, aluminium and stainless steel electrodes to make this mechanism applicable at voltage above 250 kV.

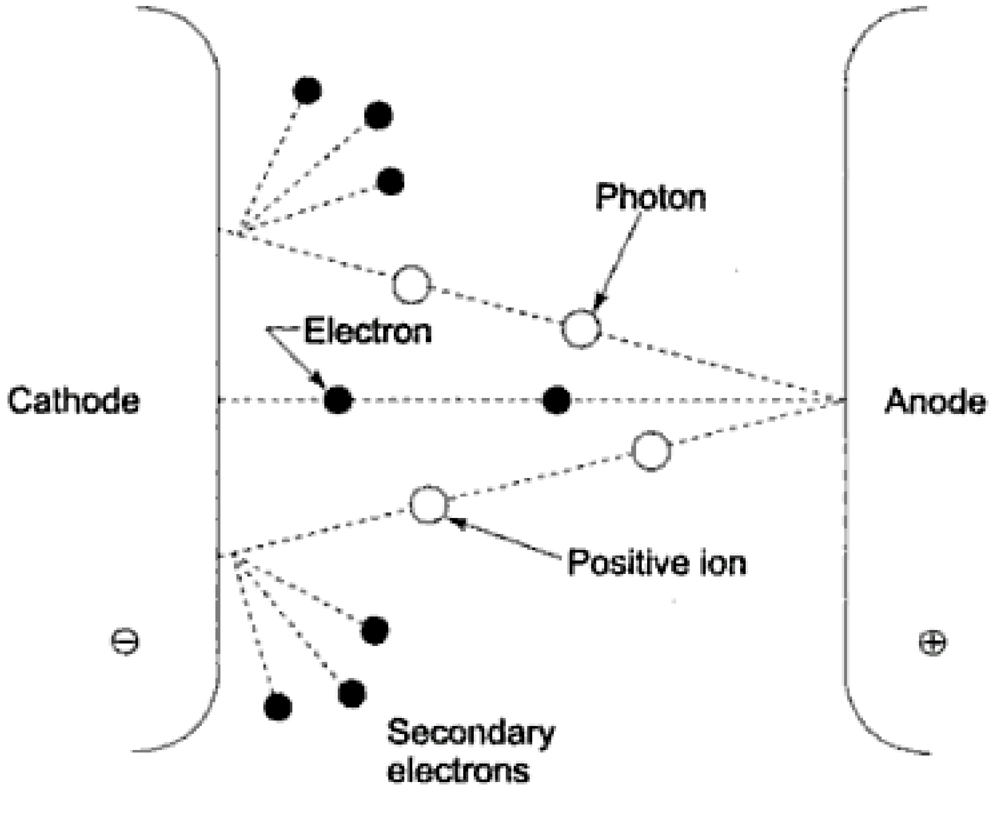

Fig. 2.22 *Particle exchange mechanism of vacuum breakdown*

(b) Field Emission Theory

(i) *Anode Heating Mechanism*

This theory postulates that electrons produced at small micro-projections on the cathode due to field emission bombard the anode causing a local rise in temperature and release gases and vapours into the vacuum gap. These electrons ionize the atoms of the gas and produce positive ions. These positive ions arrive at the cathode, increase the primary electron emission due to space charge formation and produce secondary electrons by bombarding the surface. The process continues until a sufficient number of electrons are produced to give rise to breakdown, as in the case of a low pressure Townsend type gas discharge. This is shown schematically in Fig. 2.23.

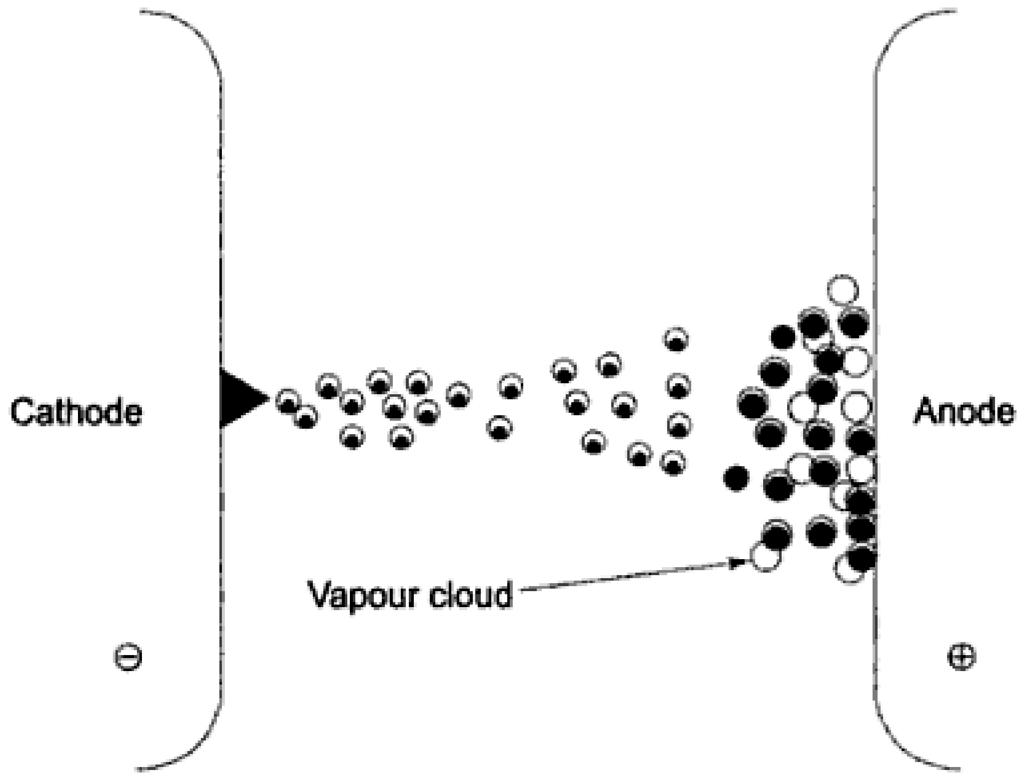

Fig. 2.23 *Electron beam anode heating mechanism of vacuum breakdown*

(ii) *Cathode Heating Mechanism*

This mechanism postulates that near the breakdown voltages of the gap, sharp points on the cathode surface are responsible for the existence of the pre-breakdown current, which is generated according to the field emission process described below.

This current causes resistive heating at the tip of a point and when a critical current density is reached, the tip melts and explodes, thus initiating vacuum discharge. This mechanism is called field emission as shown schematically in Fig. 2.24. Thus, the initiation of breakdown depends on the conditions and the properties of the cathode surface. Experimental evidence shows that breakdown takes place by this process when the effective cathode electric field is of the order of 10^6 to 10^7 V/cm.

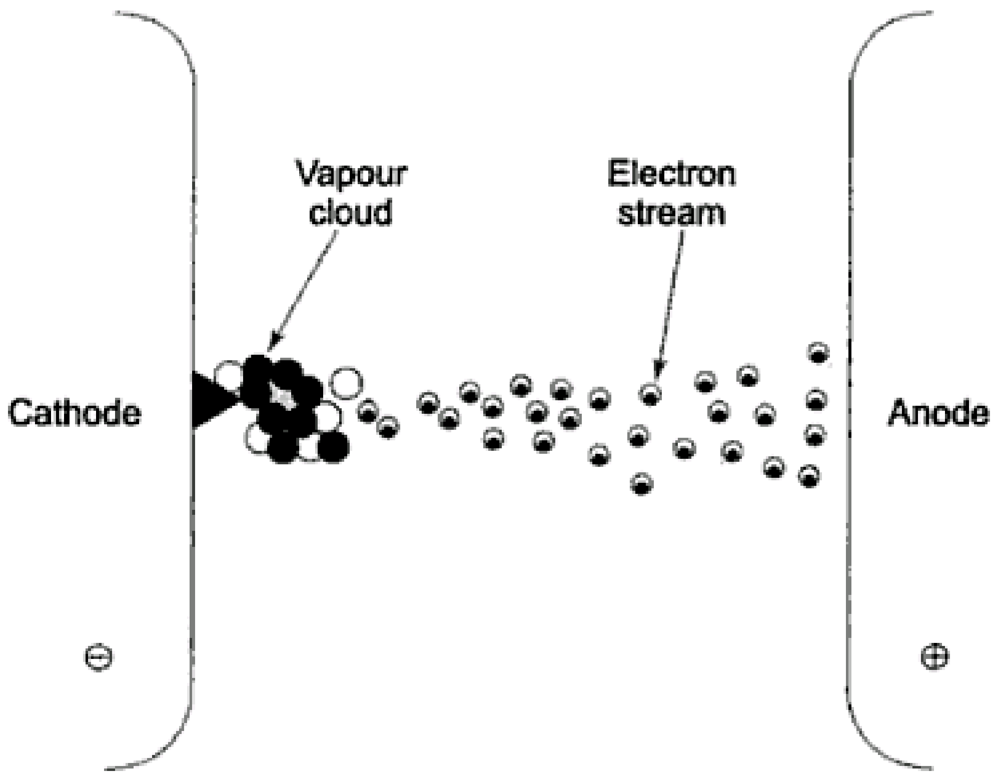

Fig. 2.24 *Breakdown in vacuum caused by the heating of a microprojection on the cathode*

(c) Clump Mechanism

Basically this theory has been developed on the following assumptions (Fig. 2.25):

(i) A loosely bound particle (clump) exists on one of the electrode surfaces.
(ii) On the application of a high voltage, this particle gets charged, subsequently gets detached from the mother electrode, and is accelerated across the gap.
(iii) The breakdown occurs due to a discharge in the vapour or gas released by the impact of the particle at the target electrode.

Cranberg was the first to propose this theory. He initially assumed that breakdown will occur when the energy per unit area, W, delivered to the target electrode by a clump exceeds a value C', a constant, characteristic of a given pair of electrodes. The quantity W is the product of gap voltage (V) and the charge density on the clump. The latter is proportional to the electric field E at the electrode of origin. The criterion for breakdown, therefore, is

$$VE = C' \tag{2.47}$$

In case of parallel plane electrodes the field $E = V/d$, where d is the distance between the electrodes. So the generalized criterion for breakdown becomes

$$V = (Cd)^{1/2} \tag{2.48}$$

where C is another constant involving C' and the electrode surface conditions.

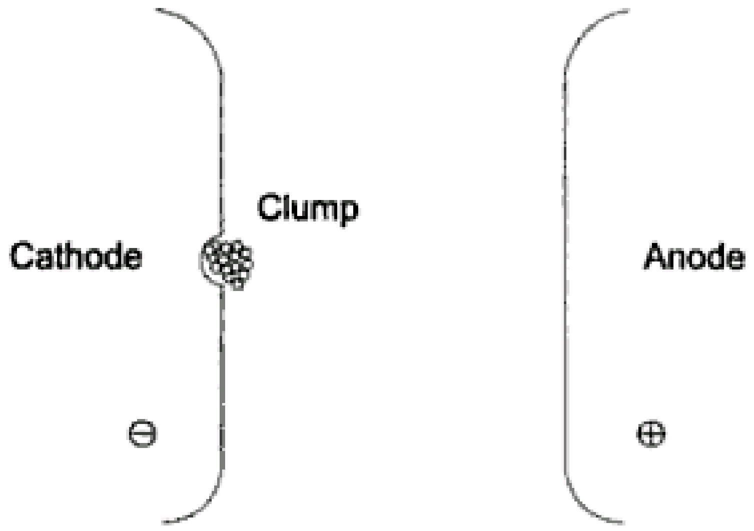

(a)
Clump is loosely attached to the surface

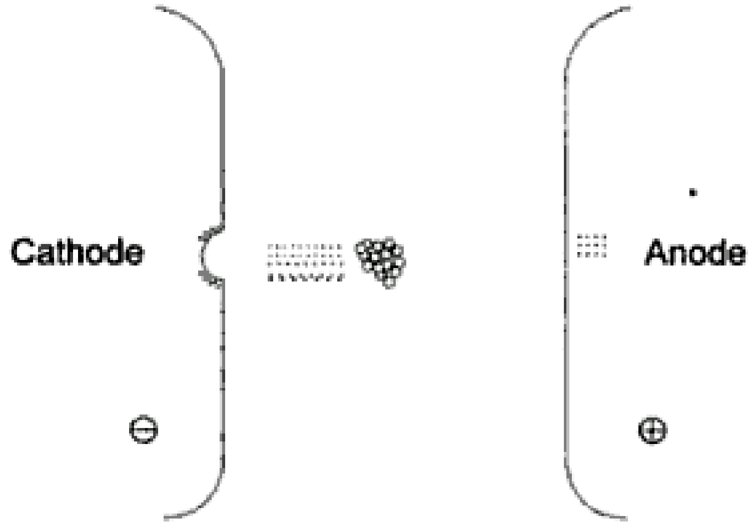

(b)
Clump is detached from the cathode surface and is accelerated across the gap

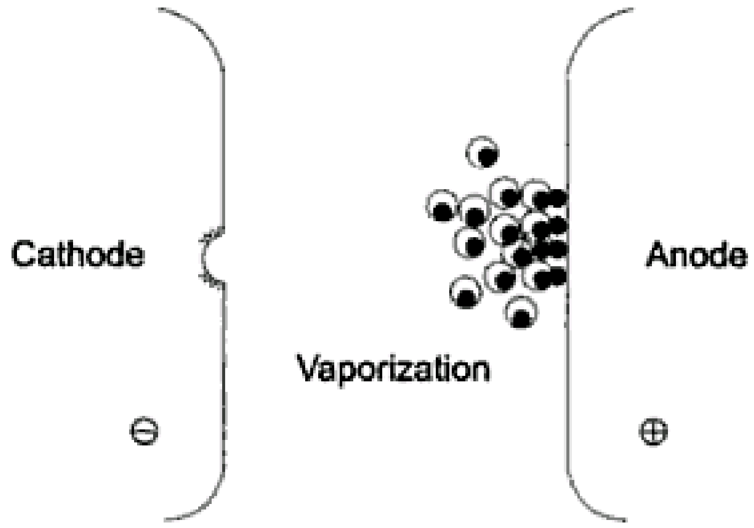

(c)
Impact of the clump on the anode gives out a cloud of metal vapour

Fig. 2.25 *(a, b, c) Clump mechanism of vacuum breakdown*

Cranberg presented a summary of the experimental results which satisfied this breakdown criterion with reasonable accuracy. He stated that the origin of the clump was the cathode and obtained a value for the constant C as 60×10^{10} V^2/cm (for iron particles). However the equation was later modified as $V = Cd^{\alpha}$, where α varies between 0.2 and 1.2 depending on the gap length and the electrode material, with a maximum at 0.6. The dependence of V on the electrode material, comes from the observations of markings on the electrode surfaces. Craters were observed on the anode and melted regions on the cathode or vice-versa after a single breakdown.

(d) Summary

Dielectric strength of vacuum is defined in different ways. In the case of vacuum insulated switchgear, it is the value of the voltage to cause the first breakdown that is important. However, when the gap breaks down repeatedly, the breakdown voltage increases with the number of breakdowns until it reaches a steady or conditioned value. This value is often taken as the breakdown strength of the vacuum gap.

Although there has been a large amount of work done on vacuum breakdown phenomena, so far, no single theory has been able to explain all the available experimental measurements and observations. Since experimental evidence exists for all the postulated mechanisms, it appears that each mechanism would depend, to a great extent, on the conditions under which the experiments were performed. The most significant experimental factors which influence the breakdown mechanism are: gap length, geometry and material of the electrodes, surface uniformity and treatment of the surface, presence of extraneous particles and residual gas pressure in the vacuum gap. It was observed that the correct choice of electrode material, and the use of thin insulating coatings on electrodes in long gaps can increase the breakdown voltage of a vacuum gap. On the other hand, an increase of electrode area or the presence of particles in the vacuum gap will reduce the breakdown voltage.

Key Terms

- Conduction and breakdown in gases
- Collusion processes
- Mobility Diffusion Coefficent
- Electron Energy Distribution
- Collusion Cross Section
- Mean Free Path
- Ionization Processes
- Primary and secondary processes
- Electron emission and attachment
- Current growth and Townsend mechanism
- Ionization coefficients
- Breakdown in gases
- Time lags
- Streamer mechanism
- Paschen's Law
- Corona discharges
- Breakdown in non-uniform fields
- Post breakdown phenomenon
- Vacuum breakdown

Worked Examples

Example 2.1 What will the breakdown strength of air be for small gaps (1 mm) and large gaps (20 cm) under uniform field conditions and standard atmospheric conditions?

Solution The breakdown strength of air under uniform field conditions and standard atmospheric conditions is approximately given by

$$E = \frac{V}{d} = \left(24.22 + \frac{6.08}{d^{1/2}}\right) \text{ kV/cm}$$

Substituting for 1 mm gap,

$$E = 24.22 + \frac{6.08}{(0.1)^{1/2}} = 43.45 \text{ kV/cm}$$

for 20 cm gap,

$$E = 24.22 + \frac{6.08}{(20.1)^{1/2}} = 25.58 \text{ kV/cm}$$

Example 2.2 In an experiment in a certain gas it was found that the steady state current is 5.5×10^{-8} A at 8 kV at a distance of 0.4 cm between the plane electrodes. Keeping the field constant and reducing the distance to 0.1 cm results in a current of 5.5×10^{-9} A. Calculate Townsend's primary ionization coefficient α.

Solution The current at the anode I is given by

$$I = I_0 \exp(\alpha d)$$

where I_0 is the initial current and d is the gap distance. Given,

$$d_1 = 0.4 \text{ cm} \qquad d_2 = 0.1 \text{ cm}$$

$$I_1 = 5.5 \times 10^{-8} \text{ A} \qquad I_2 = 5.5 \times 10^{-9} \text{ A}$$

$$\frac{I_1}{I_2} = \exp \alpha(d_1 - d_2)$$

i.e.,

$$10 = \exp(\alpha \times 0.3)$$

i.e.,

$$0.3\alpha = \ln(10) \qquad \therefore \qquad \alpha = 7.676/\text{cmer torr}$$

Multiple Choice Questions

1. Electrical conduction in gases was first studied in 1905 by
   (a) Loeb (b) Maxwell
   (c) Townsend (d) Hertz
2. According to Townsend current growth process the current (I) in a uniform electric field gap is
   (a) $I_0 e^{-\alpha d}$ (b) $I_0 e^{\alpha d}$ (c) $I_0 e^{\gamma d}$ (d) $I_0 e^{-\gamma d}$

3. The breakdown criterion in a uniform field electrode gap is
   (a) $\alpha^{-\gamma d} = 1$
   (b) $\alpha = \frac{\eta}{(1-\gamma)}$
   (c) $\gamma e^{\alpha d} = 1$
   (d) $\gamma e^{-\alpha d} = 1$
4. An electronegative gas is one in which
   (a) positive ions are formed along with electrons
   (b) the gas has inherent negative charge
   (c) gas is ionized due to electron bombardment
   (d) the gases in which electron gets attached to form negative ion.
5. SF_6 is a
   (a) neutral gas
   (b) electronegative gas
   (c) ionizes easily to form ions
   (d) non-attaching gas
6. Ionization coefficients α, γ are functions of
   (a) applied voltage
   (b) pressure and temperature
   (c) electric field
   (d) ratio of electric field to pressure.
7. Time lag for breakdown is
   (a) time difference between instant of applied voltage and occurrence of breakdown
   (b) time taken for the voltage to rise before breakdown occurs
   (c) time required for gas to breakdown under pulse application
   (d) none of the above.
8. Streamer mechanism of breakdown explains the phenomena of electrical breakdown of
   (a) very short spark gaps
   (b) when *pd* is less than 1000 torr-cm
   (c) very long gaps where field is non-uniform
   (d) spark gaps subjected to impulse voltages.
9. Paschen's law states that
   (a) breakdown voltage is a function of electric field
   (b) breakdown voltage is a function of *pd*
   (c) α and γ depends on E/p
   (d) electronegative gases have high breakdown voltage.
10. Minimum sparking potential of Air is about
    (a) 100 V (b) 4.4 kV (c) 40 V (d) 325 V
11. At standard temperature and pressure the electric field at which breakdown occur in air with a small gap *d* (cm) is given by
    (a) $30 + 6.08/d$
    (b) $24.2 + 6.08/d$
    (c) $24.2 + 6.08/\sqrt{d}$
    (d) $30d\left[1 + \frac{0.301}{\sqrt{d}}\right]$
12. For a 1 cm gap in air at 760 mm pressure and 20°C temperature the breakdown voltage is
    (a) 24 kV (b) 30.3 kV (c) 22.92 kV (d) 40 kV

13. Corona occurs before the breakdown in a sphere to ground air gap when ratio of gap distance to the radius of sphere is
    (a) > 1.0 (b) > 3.0 (c) > 10 (d) < 1.0
14. The requirement of gases for insulation purpose is
    (a) high dielectric strength and thermal stability
    (b) high dielectric strength only
    (c) high thermal stability
    (d) high thermal stability and low temperature condensation.
15. The mechanism of breakdown in vacuum is due to
    (a) Particle exchange (b) Field emission
    (c) Clump formation (d) All of the above.
16. SF_6 has the following property which is not favourable for use in electrical apparatus
    (a) high dielectric strength
    (b) high are quenching ability
    (c) it is not environmentally friendly and causes global warming
    (d) none of the above.

Answers

1. (c) 2. (b) 3. (c) 4. (d) 5. (b)
6. (d) 7. (a) 8. (c) 9. (b) 10. (d)
11. (b) 12. (b) 13. (b) 14. (a) 15. (d)
16. (d)

Review Questions

2.1 Explain the difference between photo-ionization and photo-electric emission.

2.2 Explain the term "electron attachment". Why are electron attaching gases useful for practical use as insultants when compared to non-attaching gases.

2.3 Describe the current growth phenomenon in a gas subjected to uniform electric fields.

2.4 Explain the experimental set-up for the measurement of pre-breakdown currents in a gas.

2.5 Define Townsend's first and second ionization coefficients. How is the condition for breakdown obtained in a Townsend discharge?

2.6 What are electronegative gases? Why is the breakdown strength higher in these gases compared to that in other gases?

2.7 Derive the criterion for breakdown in electronegative gases.

2.8 Explain the Streamer theory of breakdown in air at atmospheric pressure.

2.9 What are the anode and the cathode streamers? Explain the mechanism of their formation and development leading to breakdown.

2.10 What is Paschen's law? How do you account for the minimum voltage for breakdown under a given '$p \times d$' condition?

2.11 Describe the various factors that influence breakdown in a gas.

2.12 What is vacuum? How is it categorized? What is the usual range of vacuum used in high voltage apparatus?

2.13 Describ how vacuum breakdown is different from normal breakdown of a gas.

2.14 Discuss the various mechanisms of vacuum breakdown.

References

1. Meek, J.M. and Craggs, J.D., *Electrical Breakdown of Gases*, John Wiley, New York (1978).
2. Raether, H., *Electron Avalanches and Breakdown in Gases,* Butterworth, London (1964).
3. Naidu, M.S. and Maller, V.N., *Advances in High Voltage Breakdown and Arc Interruption in SF_6 and Vacuum*, Pergamon Press, Oxford (1981).
4. Nasser, E., *Fundamentals of Gaseous Ionization and Plasma Electronics*, John Wiley, New York (1974).
5. Alston, L.L., *High Voltage Technology*, Oxford University Press, Oxford (1968).
6. Kuffel, E. E., Zaengl, W.S. and Kuffel, J., *High Voltage Engineering Fundamentals* (2nd edition), Butterworth-Heinemann (2000).
7. Christophorou, L.G., *Gaseous Dielectrics*, GD-2, Pergamon Press, New York (1980).
8. Christophorou, L.G. and Dale, S.J., *Encyclopedia of Physical Science and Technology*, Edited by R.A. Mayords, **4**, pp 246–292, Academic Press, New York (1987).
9. Wurtz, M., Adam, H. and Walcher, W., *Theory and Practice of Vacuum Technology*, Fried Viewveg and Sohn, Braunswieg, Germany (1989).
10. Christophorou, L.G., Olthoff, J.K. and Green, D.S., *Gases for Electrical Insulation and Interruption: Possible, Present and Future Alternatives to Pure SF_6*, National Institute of Standards and Technology (USA), Technical Note 1425 (1997).
11. Alpert, D., *Journal of Vacuum Science and Technology*, **1**, pp 35–50 (1964).
12. R.V. Latnam, *High Voltage Vacuum Insulation,* Academic Press, London (1981).
13. Meayats, G.A. and Proskurovasky, D.L., *Pulsed Electrical Discharges in Vacuum*, Springer Verlag, Berlin, Germany (1989).

3

Conduction and Breakdown in Liquid Dielectrics

3.1 | LIQUIDS AS INSULATORS

Liquid dielectrics, because of their inherent properties, appear as though they would be more useful as insulating materials than either solids or gases. This is because both liquids and solids are usually 10^3 times denser than gases and hence, from Paschen's law it should follow that they possess much higher dielectric strength of the order of 10^7 V/cm. Also, liquids, like gases, fill the complete volume to be insulated and simultaneously will dissipate heat by convection. Oil is about 10 times more efficient than air or nitrogen in its heat transfer capability when used in transformers. Although liquids are expected to give very high dielectric strength of the order of 10 MV/cm, in actual practice the strengths obtained are only of the order of 100 kV/cm.

Liquid dielectrics are used mainly as impregnants in high voltage cables and capacitors, and for filling up of transformers, circuit breakers etc. Liquid dielectrics also act as heat transfer agents in transformers, and as arc quenching media in circuit breakers. Petroleum oils (Transformer oil) are the most commonly used liquid dielectrics. Synthetic hydrocarbons and halogenated hydrocarbons are also used for certain applications. For very high temperature application, silicone oils and fluorinated hydrocarbons are employed. However, it may be mentioned that some of the isomers of poly-chlorinated diphenyls (generally called askerels) have been found to be very toxic and poisonous, and hence, their use has been almost stopped.

Liquid dielectrics normally are mixtures of hydrocarbons and are weakly polarised. When used for electrical insulation purposes they should be free from moisture, products of oxidation and other contaminants. The most important factor that affects the electrical strength of an insulating oil is the presence of water in the form of fine droplets suspended in the oil. The presence of even 0.01% water in transformer oil reduces its electrical strength to 20% of the dry oil value. The dielectric strength of oil reduces more sharply, if it contains fibrous impurities in addition to water. Table 3.1 shows the properties of some dielectrics commonly used in electrical equipment.

Of the insulating liquids shown in Table 3.1, transformer oils are the cheapest and the most commonly used. The electrical properties of transformer oil are given in the above table. Oils used in the capacitors are similar to transformer oil but they are subjected to a very high degree of purification. Various kinds of oils are used in cables as impregnants for paper insulation and to improve their heat transfer capability. Table 3.1 gives the dielectric properties of various liquid dielectrics used in cables, capacitors and in other special applications.

In practice, the choice of a liquid dielectric for a given application is made mainly on the basis of its chemical stability. Other factors such as saving of space, cost, previous usage, and susceptibility to the environmental influences are also considered.

Table 3.1 *Dielectric Properties of Some Liquid Dielectrics*

Property	*Transformer oil*	*Cable oil*	*Capacitor oil*	*PETEP oil*	*Silicone oils*
Breakdown strength at 20°C on 2.5 mm standard sphere gap	15 kV/mm	30 kV/mm	20 kV/mm	> 15 kV/mm	30–40 kV/mm
Relative permittivity (50 Hz)	2.2–2.3	2.3–2.6	2.1	2.7	2–73
Tan δ (50 Hz)	0.001	0.002	0.25×10^{-3}	0.1×10^{-3}	10^{-3}
(1 kHz)	0.0005	0.0001	0.10×10^{-3}	0.5×10^{-3}	10^{-4}
Resistivity (ohm-cm)	10^{12}–10^{13}	10^{12}–10^{13}	10^{13}–10^{14}	$> 10^{14}$	3×10^{14}
Specific gravity at 20°C	0.89	0.93	0.88–0.89	0.96–0.97	1.0–1.1
Viscosity at 20°C (CS)	30	30	30	80	10–1000
Acid value (mg/gm of KOH)	Nil	Nil	Nil	< 0.03	Nil
Refractive index	1.4820	1.4700	1.4740	1.4555	1.5000-1.6000
Saponification (mg of KOH/gm of oil)	0.01	0.01	0.01		< 0.01
Thermal expansion (20–100°C)	7×10^{-4}/°C	7×10^{-4}/°C	7×10^{-4}/°C	0.00075	5×10^{-4}/°C
Max. permissible water content (in ppm)	50	50	50	200	< 30 (negligible)

3.1.1 Classification of Liquid Dielectrics

In recent years, a substitute to mineral oils, other polyester oils have been developed which are extensively used in transformers in Europe and other countries. One such oil is the halogen free Penta-Etythrite-Tetra Fatty Acid

Polyester oil (PETFP oil) which has very good electrical, physical and thermal properties (see Table 3.1). It is also biodegradable, i.e. when decomposed has almost negligible toxicity and does not contribute to pollution.

(a) Transformer Oil (Mineral Oil)

As already mentioned, transformer oil is the most commonly used liquid dielectric in power apparatus. It is an almost colourless liquid consisting of a mixture of hydrocarbons which include paraffins, iso-paraffins, naphthalenes and aromatics. When in service, the liquid in a transformer is subjected to prolonged heating at high temperatures of about 95°C, and consequently it undergoes a gradual ageing process. With time the oil becomes darker due to the formation of acids and resins, or sludge in the liquid. Some of the acids are corrosive to the solid insulating materials and metal parts in the transformer. Deposits of sludge on the transformer core, on the coils and inside the oil ducts reduce circulation of oil and thus its heat transfer capability gets considerably reduced. Complete specifications for the testing of transformer oils are given in IS 1866 (1983), IEC 296 (1969) and IEC 474 (1974).

(b) Synthetic Hydrocarbons

Among synthetic liquid dielectrics, polyolefins are the dielectrics of choice for applications in power cables. Over 55% of synthetic hydrocarbons produced worldwide today are polyolefins. The most commonly used olefins are polybutylene and alkylaromatic hydrocarbons (e.g., alkyl-benzene). Their general characteristics are very similar to those of mineral oils.

(c) Chlorinated Hydrocarbons

Two aromatic hydrocarbons, benzene and diphenyl, are chlorinated to produce chlorinated aromatic compounds called askarels or simply polychlorinated biphenyl (PCB). They possess high fire point and excellent electrical properties. In recent years their use has been banned throughout the world, because they pose serious health hazards.

(d) Silicone Oils

Silicone oils represent an alternative to PCBs but they are expensive. Even at a temperature of 150°C they exhibit high long-term thermal stability. Silicone oils are resistant to most chemicals, and are oxidation resistant, even at higher temperatures. They can be used at higher temperatures than mineral oils. Silicone oils are an acceptable substitute for PCBs in transformes despite their slightly inferior nonflammable properties.

(e) Esters

Natural esters such as castor oil has been used as a capacitor impregnant for many years, but currently two types of synthetic esters are being used, viz. organic esters and phosphate esters.

Organic esters have high boiling points in relation to their viscosity and, therefore, have high fire points. They have a good viscosity-temperature relationship and are used extensively in capacitors.

The phosphate esters have high boiling point and low flammability and therefore are used in transformers that are to be installed in hazardous areas.

(f) Latest Developments

Some new oils have been introduced in recent years. These are being marketed under different commercial names, such as high temperature hydrocarbon oil, tetrachloroethylene and perfluoropolyether.

High Temperature Hydrocarbon (HTH) oils have good electrical insulating and adequate heat transfer properties. They are chemically similar to regular mineral transformer oils, but possess higher boiling points and higher fire points. However, they have higher viscosity which reduces heat transfer capability.

Table 3.2 *Properties of High Temperature Hydrocarbons (HTH) Oils and Tetrachloroethylene (C_2Cl_4)*

Property	*HTH*	C_2Cl_4
Dielectric strength, kV	43	43
Impulse breakdown, kV		
Negative polarity	118	—
Positive polarity	85	—
Dielectric constant, ε_r	2.38	2.365
Dissipation factor (%)		
100°C	0.4	—
50°C	0.4	0.05
25°C	$< 10^{-3}$	—
Flach point, °C	285	none
Fire point, °C	312	none
Pour point, °C	–30	–22
Viscosity, *cSt*		
100°C	16	0.36
50°C	85	0.42
25°C	350	0.55
Specific gravity, g/cm^3	0.877	1.620

Tetrachloroethylene (C_2Cl_4) is a nonflammable insulating fluid, and is used in mixtures with mineral oil. It has very low viscosity and therefore gives excellent heat transfer properties. Some typical properties of HTH oil and C_2Cl_4 are given below in Table 3.2. Perfluoropolyether has been recently introduced in the European market with the trade name Galden HT40. It is a nonflammable oil and its boiling point exceeds 400°C. It possesses low vapour pressure, so can be used as a good heat transfer medium.

3.1.2 Characteristics of Liquid Dielectrics

Essentially a liquid dielectric should possess good dielectric properties, excellent heat transfer characteristics and must be chemically stable under the range of conditions under which the equipment operates. These are briefly discussed below.

(a) Electrical Properties

The electrical properties that are essential in determining the dielectric performance of a liquid dielectric are

(i) its capacitance per unit volume or its relative permittivity
(ii) its resistivity
(iii) its loss tangent (tan δ) or its power factor which is an indication of the power loss under a.c. voltage application
(iv) its ability to withstand high electric stresses.

Permittivities of most of the petroleum oils vary from 2.0 to 2.6 while those of silicone oils from 2.0 to 73 (see Table 3.1). In case of the non-polar liquids, the permittivity is independent of frequency but in the case of polar liquids, such as water, it changes with frequency. For example, the permittivity of water is 78 at 50 Hz and reduces to about 5.0 at 1 MHz.

Resistivities of insulating liquids used for high voltage applications should be more than 10^{16} ohm-metre and most of the liquids in their pure state exhibit this property.

Power Factor of a liquid dielectric under a.c. voltage will determine its performance under load conditions. Power factor is a measure of the power loss and is an important parameter in cable and capacitor systems. However, in the case of transformers, the dielectric loss in the oil is negligible when compared to copper and iron losses. Pure and dry transformer oil will have a very low power factor varying between 10^{-4} at 20°C and 10^{-3} at 90°C at a frequency of 50 Hz.

Dielectric Strength is the most important parameter in the choice of a given liquid dielectric for a given application. The dielectric strength depends on the atomic and molecular properties of the liquid itself. However, under practical conditions the dielectric strength depends on the material of the electrodes, temperature, type of applied voltage, gas content in the liquid etc., which change the dielectric strength by changing the molecular properties of the liquid. The above factors which control the breakdown strength and leads to electrical breakdown of the liquid dielectrics.

(b) Heat Transfer Characteristics

In equipments filled with a liquid dielectric (transformer, cable, circuit breaker, etc.), heat is transferred mainly by convection. Under natural atmospheric cooling conditions convection (N) is given by

$$N = f\,[K^3\,AC/v]^n \tag{3.1}$$

where K = thermal conductivity, A = coefficient of expansion, C = specific heat per unit volume, v = kinematic viscosity, and $n = 0.25 \sim 0.33$. The main factors that control the heat transfer are thermal conductivity (K) and viscosity (v). From Eq. (3.1) it can be seen that a higher value for K is preferable for apparatus likely to operate continuously at a high temperature. On the other hand, a low value of K and high viscosity can lead to localized overheating or even electrical "burn out".

Silicone oils do not exhibit these properties and therefore can pose severe overheating problems in equipment that use these dielectric oils.

(c) Chemical Stability

In service, insulating liquids are subjected to thermal and electrical stresses in the presence of materials like O_2, water, fibres and decomposition products of solid insulation. These, either singly or in combination, cause degradation of the liquid with the result that soluble solid and gaseous products are found, which can result in corrosion, impairment of heat transfer, deterioration of electrical properties, increased dielectric losses, discharges and arcing. In the absence of any remedial action, this cycle continues and produces an ever-worsening liquid purity and equipment condition.

3.2 | PURE LIQUIDS AND COMMERCIAL LIQUIDS

Pure liquids are those which are chemically pure and do not contain any other impurity even in traces of 1 in 10^9, and are structurally simple. Examples of such simple pure liquids are n-hexane (C_6H_{14}), n-heptane (C_7H_{16}) and other paraffin hydrocarbons. By using simple and pure liquids, it is easier to separate out the various factors that influence conduction and breakdown in them. On the other hand, the commercial liquids which are insulating liquids like oils which are not chemically pure, normally consist of mixtures of complex organic molecules which cannot be easily specified or reproduced in a series of experiments.

3.2.1 Purification

The main impurities in liquid dielectrics are dust, moisture, dissolved gases and ionic impurities. Various methods employed for purification are filtration (through mechanical filters, spray filters, and electrostatic filters), centrifuging, degassing and distillation, and chemical treatment (adding ion exchange materials such as alumina, fuller's earth, etc. and filtering). Dust particles when present become charged and reduce the breakdown strength of the liquid dielectrics, and they can be removed by careful filtration. Liquid will normally contain moisture and dissolve gases in small quantities. Gases like oxygen and carbon dioxide significantly affect the breakdown strength of the liquids, and hence it is necessary to control the amount of gas present. This is done by distillation and degassing. Ionic impurity in liquids, like water vapour which easily dissociates, leads to very high conductivity and heating of the liquid depending on the applied electric field. Water is removed using drying agents or by vacuum drying. Sometimes, liquids are shaken with concentrated sulphuric acid to remove wax and residue and washed with caustic soda and distilled water. A commonly used closed-cycle liquid purification system to prepare liquids as per the above requirements is shown in Fig. 3.1. This system provides for cycling the liquid. The liquid from the reservoir flows through the distillation column where ionic impurities are removed. Water is removed by drying agents or frozen out in the low-temperature bath. The gases dissolved in the liquid are removed by passing them through the cooling tower and/or pumped out by the vacuum pumps. The liquid then passes through the filter where dust particles are removed. The liquid thus purified is then used in the test cell. The used liquid then flows back into the reservoir. The vacuum system thus helps to remove the moisture and other gaseous impurities.

3.2.2 Breakdown Tests

Breakdown tests are normally conducted using test cells. For testing pure liquids, the test cells used are small so that less quantity of liquid is used during testing. Also, test cells are usually an integral part of the purification system as shown in Fig. 3.1. The electrodes used for breakdown voltage measurements are usually spheres of 0.5 to 1 cm in diameter with gap spacings of about 100–200 μm. The gap is accurately controlled by using a micrometer. Sometimes parallel plane uniform-field electrode systems are also used. Electrode separation is very critical in measurements with liquids, and also the electrode surface smoothness and the presence of oxide films have a marked influence on the breakdown strength. The test voltages required for these tests are usually low, of the order of 50–100 kV, because of small electrode spacings. The breakdown strengths and d.c. conductivities obtained in pure liquids are very high, of the order of 1 MV/cm and 10^{-18}–10^{-20} mho/cm respectively, the conductivity being measured at electric fields of the order of 1 kV/cm. However, the corresponding values in commercial liquids are relatively low, as can be seen from Table 3.1.

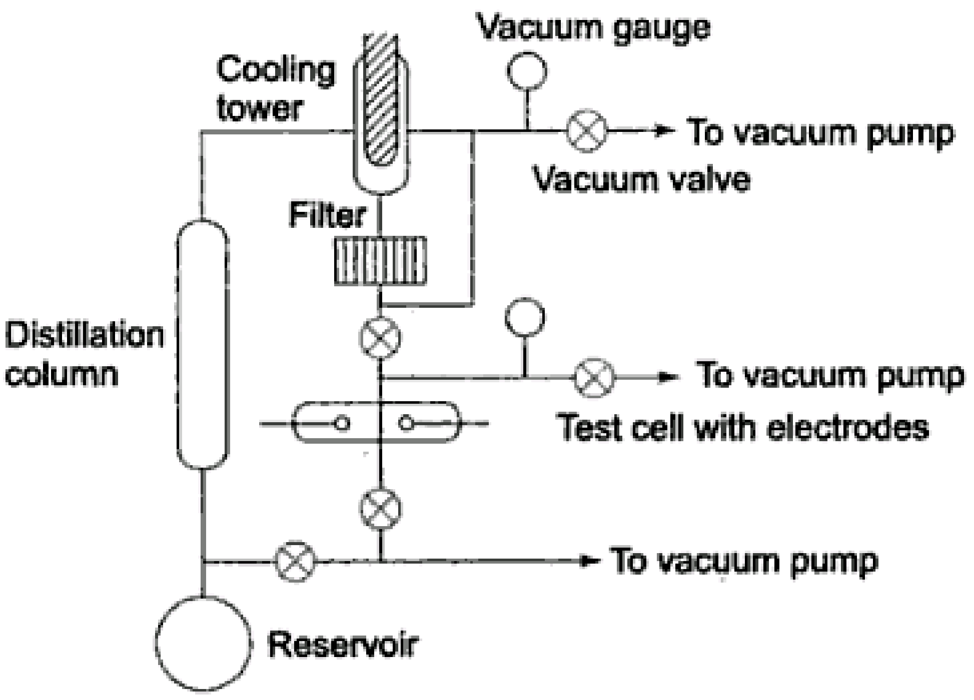

Fig. 3.1 *Liquid purification system with test cell*

3.3 | CONDUCTION AND BREAKDOWN IN PURE LIQUIDS

When low electric fields less than 1 kV/cm are applied, conductivities of 10^{-18}–10^{-20} mho/cm are obtained. These are probably due to the impurities remaining after purification. However, when the fields are high (> 100 kV/cm) the currents not only increase rapidly, but also undergo violent fluctuations which will die down after some time. A typical mean value of the conduction current in hexane is shown in Fig. 3.2.

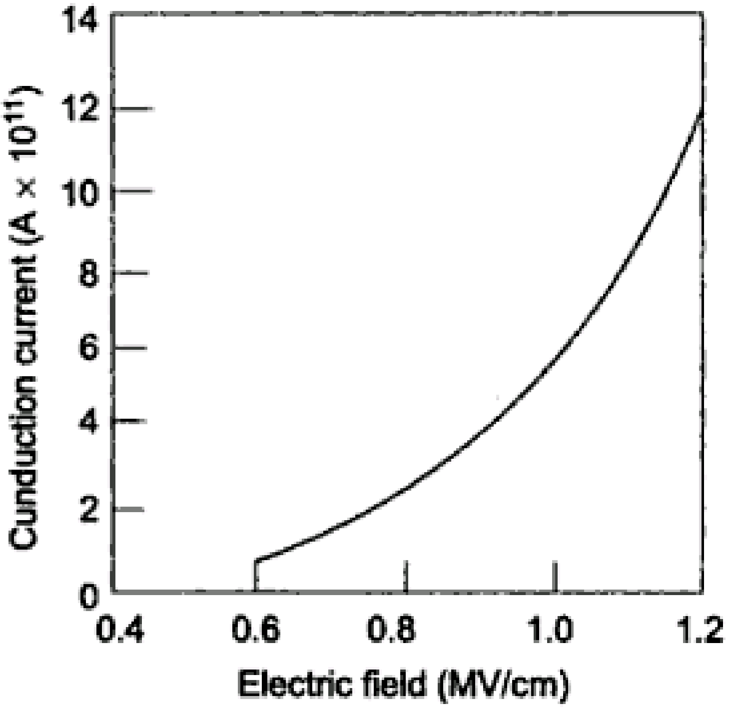

Fig. 3.2 *Conduction current-electric field characteristic in hexane at high fields*

This is the condition nearer to breakdown. However, if this figure is redrawn starting from very small currents, a current-electric field characteristic as shown in Fig. 3.3, can be obtained. This curve will have three distinct regions as shown. At very low fields the current is due to the dissociation of ions. With intermediate fields the current reaches a saturation value, and at high fields the current generated because of the field-aided electron emission from the cathode gets multiplied in the liquid medium by a Townsend type of mechanism (see Chapter 2). The current multiplication also occurs from the electrons generated at the interfaces of liquid and impurities. The increase in current by these processes continues till breakdown occurs.

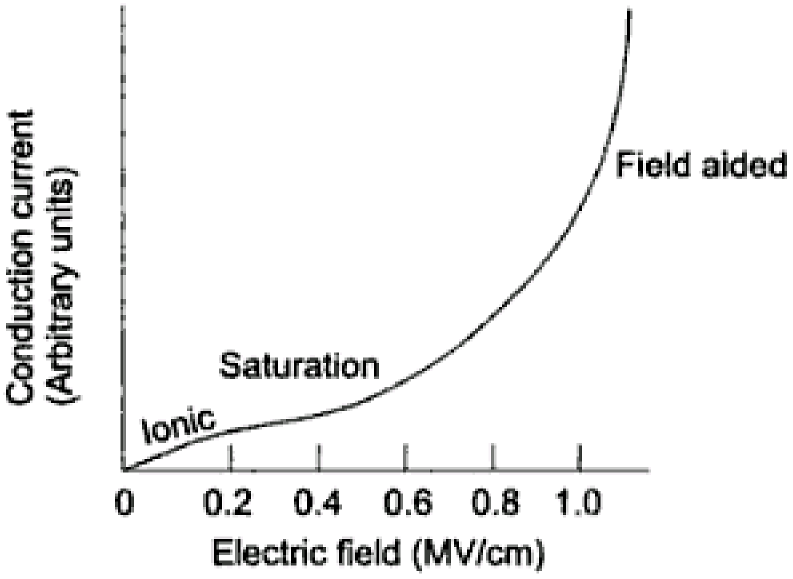

Fig. 3.3 *Conduction current-electric field characteristic in a hydrocarbon liquid*

The exact mechanism of current growth is not known; however, it appears that the electrons are generated from the cathode by field emission of electrons. The electrons so liberated get multiplied by a process similar to Townsend's primary and secondary ionization in gases (see Chapter 2, Secs 2.2 to 2.5). As the breakdown field is approached, the current increases rapidly due to a process

Table 3.3 *Maximum Breakdown Strengths of Some Liquids*

Liquid	*Maximum breakdown strength (MV/cm)*
Hexane	1.1–1.3
Benzene	1.1
Transformer oil	1.0
Silicone	1.0–1.2
Liquid Oxygen	2.4
Liquid Nitrogen	1.6–1.9
Liquid Hydrogen	1.0
Liquid Helium	0.7
Liquid Argon	1.10–1.42

similar to the primary ionization process and also the positive ions reaching the cathode generate secondary electrons, leading to breakdown. The breakdown voltage depends on the field, gap separation, cathode work-function, and the temperature of the cathode. In addition, the liquid viscosity, the liquid temperature, the density, and the molecular structure of the liquid also influence the breakdown strength of the liquid. Typical maximum breakdown strengths of some highly purified liquids and liquefied gases are given in Table 3.3.

It has been observed that the increase in breakdown strength is more, if the dissolved gases are electronegative in character (like oxygen).

Similarly, the increase in the liquid hydrostatic pressure increases the breakdown strength. These properties are shown in Figs 3.4 and 3.5.

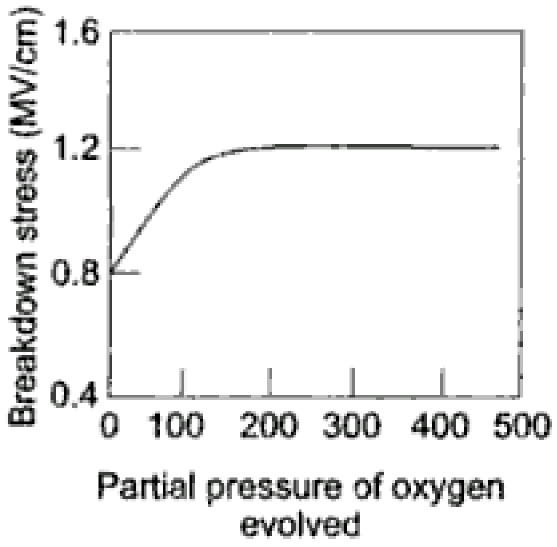

Fig. 3.4 *Effect of oxygen gas evolved on the breakdown stress in n-hexane*

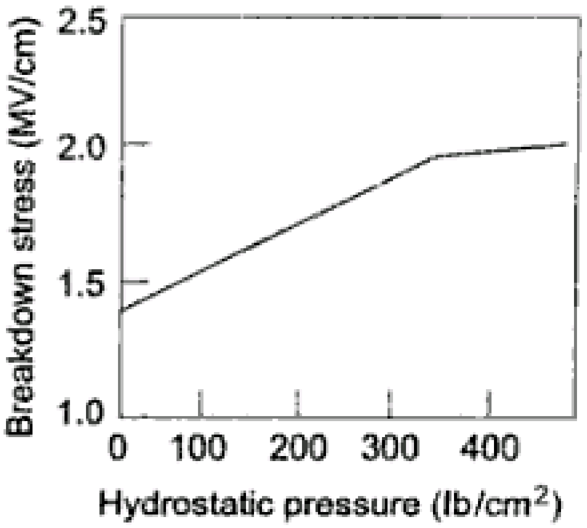

Fig. 3.5 *Effect of hydrostatic pressure on breakdown stress in n-hexane*

To sum up, this type of breakdown process in pure liquids, called the electronic breakdown, involves emission of electrons at fields greater than 100 kV/cm. This emission occurs either at the electrode surface irregularities or at the interfaces of impurities and the liquid. These electrons get further multiplied by Townsend's type of primary and secondary ionization processes, leading to breakdown.

3.4 CONDUCTION AND BREAKDOWN IN COMMERCIAL LIQUIDS

As already mentioned, commercial insulating liquids are not chemically pure and have impurities like gas bubbles, suspended particles, etc. These impurities reduce the breakdown strength of these liquids considerably. The breakdown mechanisms are also considerably influenced by the presence of these impurities. In addition, when breakdown occurs in these liquids, additional gases and gas bubbles are evolved and solid decomposition products are formed. The electrode surfaces become rough, and at times explosive sounds are heard due to the generation of impulsive pressure through the liquid.

The breakdown mechanism in commercial liquids is dependent, as seen above, on several factors, such as the nature and condition of the electrodes, the physical properties of the liquid, and the impurities and gases present in the liquid. Several theories have been proposed to explain the breakdown in liquids, and they are classified as follows:

(a) Suspended Particle Mechanism
(b) Cavitation and Bubble Mechanism
(c) Stressed Oil Volume Mechanism

These are explained briefly below.

3.4.1 Suspended Particle Theory

In commercial liquids, the presence of solid impurities cannot be avoided. These impurities will be present as fibres or as dispersed solid particles. The permittivity of these particles (ε_2) will be different from the permittivity of the liquid (ε_1). If we consider these impurities to be spherical particles of radius r, and if the applied field is E, then the particles experience a force F, where

$$F = \frac{1}{2r^3}\frac{(\varepsilon_2 - \varepsilon_1)}{2\varepsilon_1 + \varepsilon_2} \text{ grad } E^2 \tag{3.2}$$

This force is directed towards areas of maximum stress, if $\varepsilon_2 > \varepsilon_1$, for example, in the case of the presence of solid particles like paper in the liquid. On the other hand, if only gas bubbles are present in the liquid. i.e. $\varepsilon_2 < \varepsilon_1$, the force will be in the direction of areas of lower stress. If the voltage is continuously applied (d.c.) or the duration of the voltage is long (a.c.), then this force drives the particles towards the areas of maximum stress. If the number of particles present are large, they become aligned due to these forces, and thus form a stable chain bridging the electrode gap causing a breakdown between the electrodes.

If there is only a single conducting particle between the electrodes, it will give rise to local field enhancement depending on its shape. If this field exceeds the breakdown strength of the liquid, local breakdown will occur near the particle, and this will result in the formation of gas bubbles which may lead to the breakdown of the liquid.

The values of the breakdown strength of liquids containing solid impurities was found to be much less than the values for pure liquids. The impurity particles reduce the breakdown strength, and it was also observed that the larger the size of the particles the lower were the breakdown strengths.

3.4.2 Cultivation and the Bubble Theory

It was experimentally observed that in many liquids, the breakdown strength depends strongly on the applied hydrostatic pressure, suggesting that a change of phase of the medium is involved in the breakdown process, which in other words means that a kind of vapour bubble formed is responsible for breakdown. The following processes have been suggested to be responsible for the formation of the vapour bubbles:

(a) gas pockets at the surfaces of the electrodes;
(b) electrostatic repulsive forces between space charges which may be sufficient to overcome the surface tension;
(c) gaseous products due to the dissociation of liquid molecules by electron collisions; and
(d) vapourization of the liquid by corona type discharge from sharp points and irregularities on the electrode surfaces.

Once a bubble is formed it will elongate in the direction of the electric field under the influence of electrostatic forces. The volume of the bubble remains constant during elongation. Breakdown occurs when the voltage drop along the length of the bubble becomes equal to the minimum value on the Paschen's curve (see Chapter 2, Sec. 2.10) for the gas in the bubble. The breakdown field is given as

$$E_0 = \frac{1}{(\varepsilon_1 - \varepsilon_2)} \left[\frac{2\pi\sigma(2\varepsilon_1 + \varepsilon_2)}{r} \left\{ \frac{\pi}{4} \sqrt{\left(\frac{V_b}{2rE_0} \right)} - 1 \right\} \right]^{1/2} \tag{3.3}$$

where σ is the surface tension of the liquid, ε_1 is the permittivity of the liquid, ε_2 is the permittivity of the gas bubble, r is the initial radius of the bubble assumed as a sphere and V_b is the voltage drop in the bubble (corresponding to minimum on the Paschen's curve). From this equation, it can be seen that the breakdown strength depends on the initial size of the bubble which in turn is influenced by the hydrostatic pressure and temperature of the liquid.

This theory does not take into account the production of the initial bubble and hence the results given by this theory do not agree well with the experimental results. This is shown in Fig. 3.6.

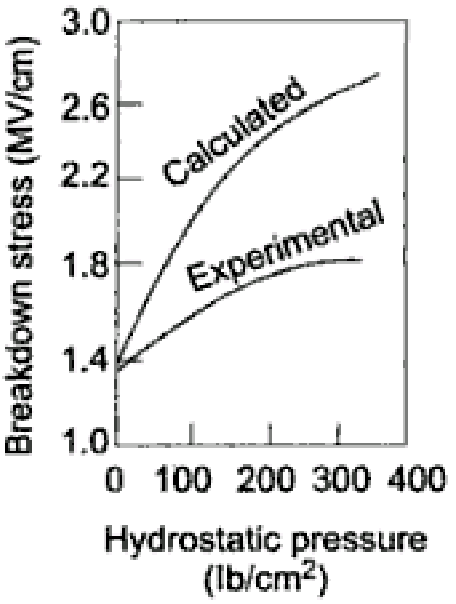

Fig. 3.6 *Theoretical and experimental breakdown stresses in n-hexane*

3.4.3 Thermal Mechanism of Breakdown

Another mechanism proposed to explain breakdown under pulse conditions is thermal breakdown. This mechanism is based on the experimental observations of extremely large currents just before breakdown. This high current pulses are believed to originate from the tips of the microscopic projections on the cathode surface with densities of the order of 1 A/cm^3. These high density current pulses give rise to localised heating of the oil which may lead to the formation of vapour